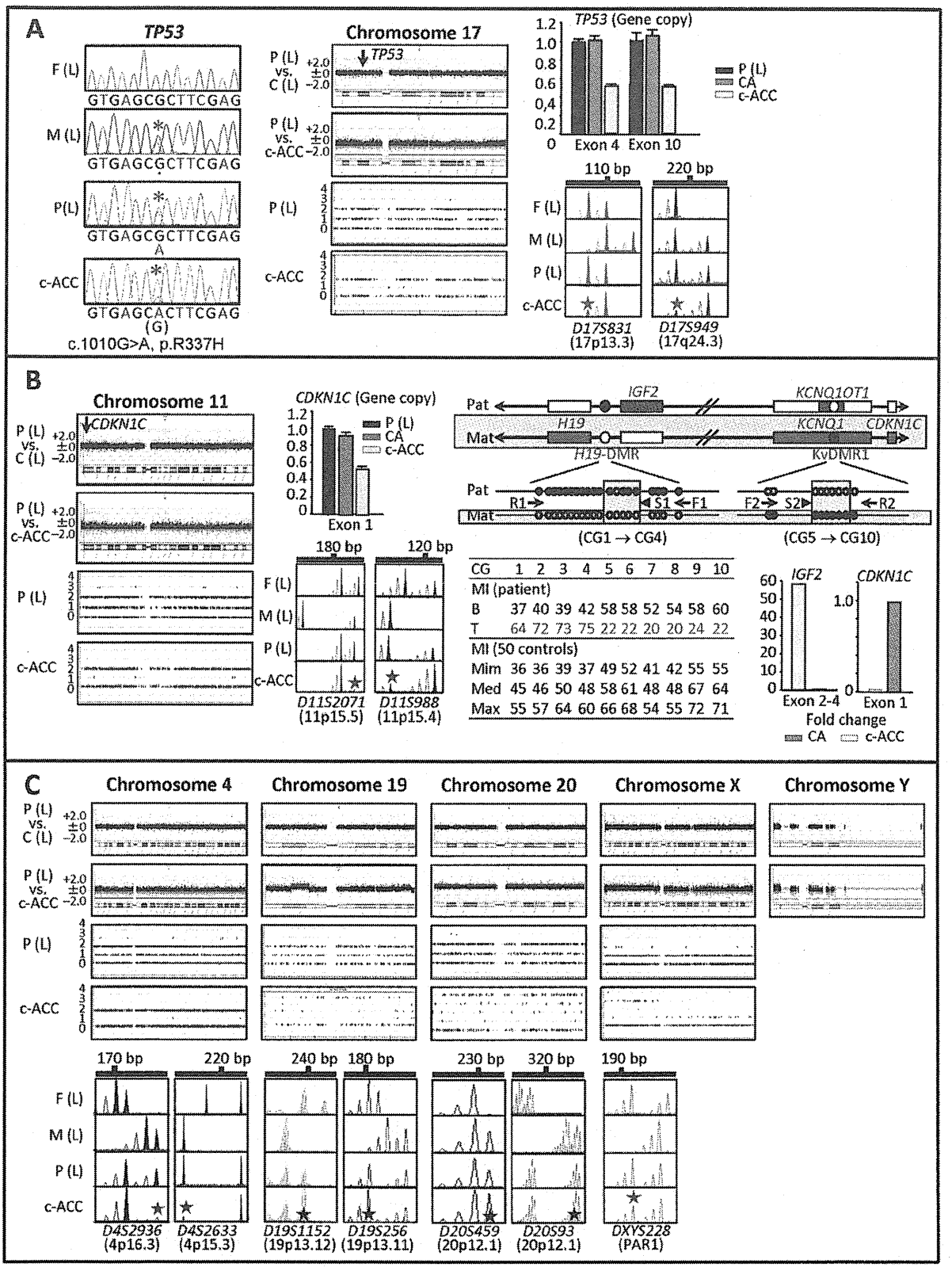

Fig. 3. Representative molecular findings. F (L): father's leukocyte genomic DNA; M (L): mother's leukocyte genomic DNA; P (L): patient's leukocyte genomic DNA; C (L): control male's leukocyte genomic DNA; c-ACC: patient's tumor genomic DNA, and CA: patient's control adrenal genomic DNA. The red and blue star symbols on the microsatellite data indicate decreased and increased peaks in the c-ACCs, respectively. For the aCGH and SNP array findings, see below. A. Germline *TP53* p.P337H (c.1010G > A) mutation of maternal origin (indicated by red asterisks) and loss of paternally inherited chromosome 17 with wildtype *TP53* from the c-ACC. B. Loss of maternally derived chromosome 11 from the c-ACC. In the upper right figure indicating the chromosome 11p15.5 imprinted regions, paternally and maternally expressed genes are shown in blue and red, respectively; filled and open circles denote methylate and unmethylated CpG dinucleotides, respectively. Deleted alleles of maternal origin are indicated with gray

paternally inherited chromosome 17 with the wildtype *TP53* from the c-ACC (Fig. 3A). In this regard, the results obtained using the c-ACC genomic DNA, such as the minor *TP53* "G" allele in direct sequencing and the minor peaks for paternally derived alleles in microsatellite analysis, were considered to derive from contaminated non-tumor tissue.

aCGH and SNP array analyses, qPCR for *CDKN1C*, and microsatellite analysis also delineated loss of the whole chromosome 11 of maternal origin in virtually all the c-ACC cells, with the trace of contaminated non-tumor tissue (Fig. 3B). In agreement with this, pyrosequencing-based methylation analysis revealed the hypermethylated *H19*-DMR and the hypomethylated KvDMR1 in the c-ACC, and qPCR analysis showed marked hyperexpression of *IGF2* and drastic hypoexpression of *CDKN1C* (Fig. 3B).

aCGH, SNP array, and microsatellite analyses also delineated loss of the whole chromosome 4 of maternal origin and copy number gains of the middle part of chromosome 19p of paternal origin in actually all the c-ACC cells (Fig. 3C). Furthermore, such analyses indicated complex rearrangements including copy number gains and losses of the distal part of chromosome 19q, copy number gains of the whole chromosome 20 of maternal origin, copy number gains of most of the Xp, and copy number losses of most of the Xq and the whole Y in a substantial fraction of the c-ACC cells (Fig. 3C). The copy number gains of maternally derived chromosome 20 were also supported by methylation analysis (Supplementary Table 3). In addition, variable degrees of copy number alterations were also implicated for chromosomes 1, 5, 7, 8, 14, and 15 in a certain fraction of the c-ACC cells by aCGH, SNP array, and methylation analyses.

3.5. Expression patterns of putative carcinogenic genes for ACTs

No significant alterations (fold change, >2.0 or <0.5) was identified for *CTNNB1, GNAS, ZNRF3*, and *KREMEN1* by DNA chip analysis.

4. Discussion

We studied steroid metabolite profiles and gene expression patterns in the c-ACC of this Brazilian boy. The expression data imply that the c-ACC has steroidogenic properties of not only fetal adrenal but also Leydig cells, because the c-ACC was associated with (i) high *CYP11A1* and *CYP17A1* expressions common to both fetal adrenal and Leydig cells, (ii) severely reduced *HSD3B2* expression and obviously high *SULT2A1* expression indicative of fetal adrenal character, and (iii) markedly high *HSD17B3* expression and a demonstrable level of *INSL3* expression characteristic of Leydig cells [15,23]. This notion would explain why the c-ACC was capable of producing not only abundant DHEA/DHEA-S but also a large amount of T primarily via the Δ5 pathway, with Δ5A-diol rather than Δ4A-dione being the primary intermediate metabolite.

Such combined steroidogenic characters of fetal adrenal and Leydig cells have also been reported in testicular adrenal rest tumors (TARTs) in males [24]. In this regard, steroidogenic cells in the fetal adrenal and the gonad are derived from the common ancestors, and human fetal adrenal cells appear to express both *AKR1C3* and *HSD17B3* around 8–9 weeks post conception [25]. It would be possible, therefore, that ACTs and TARTs may have acquired pluripotential steroidogenic functions that have once been exhibited by the common ancestral cells. Furthermore, since serum T is also increased in virilizing girls with c-ACCs [11], c-ACCs in girls may also have acquired Leydig cell-like property.

Several findings should be pointed out with regard to the steroidogenic characters. First, the conversion from 17-OHP5 to DHEA and that from 17-OHP4 to Δ4A-dione were rather compromised in the c-ACC. This would primarily be due to the relatively low 17/20 lyase activity as compared with 17α-hydroxylase activity of CYP17A1 [26], and relatively low expression of *CYB5A* required for the 17/20 lyase function [15]. Furthermore, since DHEA would efficiently be converted into DHEA-S and Δ5A-diol, this would result in a drastic difference between 17-OHP5 and DHEA concentrations within the c-ACC. Second, the conversion from 17-OHP5 to 17-OHP4 and that from Δ5A-diol to T were apparently well preserved despite the weak *HSD3B2* expression in the c-ACC. This may be explained by assuming that accumulation of a large amount of substrates maximally stimulated the residual HSD3B2 activity, especially for the conversion from Δ5A-diol to T in the c-ACC with a character of Leydig cells that produce T as the final bioactive product. Third, steroid metabolite profile was considerably different between the c-ACC and the serum. This would not be surprising, because serum steroid metabolites derive from not only the c-ACC but also extratumoral tissues. Furthermore, it is likely that intermediate metabolites such as 17-OHP5 are just leaked from the c-ACC to the blood flow, whereas biologically important metabolites such as DHEA/DHEA-S involved in the feto-placental unit [15] are positively secreted into the blood flow. Lastly, the backdoor pathway was not operating in the c-ACC.

We also attempted to reveal underlying carcinogenic factors of the c-ACC in this patient (Supplementary Fig. 3). Notably, of the genetic aberrations identified in virtually all the c-ACC cells of this patient, loss of chromosomes 17 with a wildtype *TP53*, and loss of maternally inherited chromosome 11 and resultant marked hyperexpression of *IGF2* and drastic hypoexpression of *CDKN1C*, have been detected in most, if not all, of *TP53* mutation positive c-ACCs [7]. In this context, loss of the maternally derived

boxes. For methylation analysis of the *H19*-DMR, a segment encompassing 21CpG dinucleotides was PCR-amplified with F1 & R1 primers, and a sequence primer (S1) was hybridized to a single-stranded PCR products. Subsequently, the methylation indices (MIs, the ratio of methylated clones) were obtained for four CpG dinucleotides (CG1–CG4) (indicated with a green rectangle). The KvDMR1 was similarly examined using F2 & R2 primers and S2, and the MIs were obtained for CG5–CG10. C. Copy number alterations of chromosomes 4, 19, 20, X, and Y. For chromosome 19p, the relative ratio of the area under curves (AUCs) between the two peaks is: *D19S1152*, 1.0:0.83 for P (L) and 1.0:1.76 for c-ACC; and *D19S256*, 1.37:1.0 for P (L) and 2.45:1.0 for c-ACC. The results, together with those of aCGH and SNP array, indicate duplication of paternally derived alleles in virtually all the c-ACC cells. Similar analyses, including the comparison of the AUCs between P (L) and c-ACC, implicate copy number gains of maternally inherited chromosome 20, copy number gains of the Xp, copy number reductions of the Xq, and copy number reductions of the Y chromosome including the short arm pseudoautosomal region (PAR1), in a substantial fraction of the c-ACC cells. **Note for the aCGH and SNP array findings** In aCGH for autosomes, the black, the red, and the green dots denote signals indicative of the normal, the increased ($\log_2$ signal ratio > +0.4), and the decreased ($\log_2$ signal ratio <−0.8) copy numbers, respectively; for sex chromosomes that appear in a heterogametic condition in a male, duplication leads to the $\log_2$ signal ratios of +2.0, and deletion results in the $\log_2$ signal ratios of $-\infty$ (thus, the $\log_2$ signal ratios for Xp, Xq, and Y chromosomes in this boy indicate the occurrence of copy number alterations in a substantial fraction of the c-ACC cells rather than in most of the c-ACC cells). In SNP array for autosomes, the dots for $\log_2$ signal ratios of "0 or 2" and "1" denote homozygous and heterozygous regions, respectively, and those for $\log_2$ signal ratios of "3" and "4" represent regions of increased copy numbers. Thus, the presence of the signals for "0 or 2" and the absence of those for "1" indicate hemizygosity (loss of heterozygosity) or full isodisomy. For the X chromosome in a male, the $\log_2$ signal ratio of "0" and "1" denote the hemizygosity for corresponding regions, and that of "3" represent the three copies of the .corresponding regions.

chromosome 11 would have played a major role in the carcinogenic process, by providing a drastic growth potential. Indeed, *CDKN1C* is strongly expressed in the adrenal, and gain-of-function mutations of *CDKN1C* lead to IMAGe syndrome with adrenal aplasia/hypoplasia [27], whereas loss-of-function mutations of *CDKN1C* result in Beckwith-Wiedemann syndrome characterized by the frequent occurrence of c-ACTs [28]. Furthermore, *IGF2* expression was markedly increased, probably due to loss of functional *CDKN1C* in the c-ACTs [7,29]. In addition, loss of chromosome 4 and copy number gain of the middle part of 19p have also frequently been identified in *TP53* mutation positive c-ACCs [6]. By contrast, the c-ACC of this patient was free from altered expression dosages of *CTNNB1, GNAS, ZNRF3*, and *KREMEN1*, as in most *TP53* mutation positive c-ACCs [6,7]. Thus, fairly common carcinogenic factors appear to be operating in *TP53* mutation positive c-ACCs.

See Excel sheet 1 as supplementary file. Supplementry material related to this article found, in the online version, at http://dx.doi.org/10.1016/j.jsbmb.2016.02.031.

The experiments using the H295R cells also provide useful implications. It is likely that the H295R cells basically have steroidogenic characters of fetal adrenal and the zona fasciculata and the zona reticularis of permanent adrenal, although they have barely contained CYP11B1 activity. Thus, the H295R cells, as well as the c-ACC, appear to have acquired pluripotential steroidogenic functions. In this regard, the difference in steroid metabolite profile including the T and cortisol values between the H295R cells and the c-ACC would be due to the difference in the original tissue and the underlying carcinogenic factors. While T production in the H295R cells was severely compromised despite the presence of a relatively high *AKR1C3* expression, previous studies have shown that H295A cells are virtually incapable of producing T despite *AKR1C3* expression level being similar to that of H295R cells [30]. Thus, adrenal T production would be subject to some factors other than the *AKR1C3* expression level. Furthermore, the discrepancy in steroid metabolite values between the H295R cells and the media would argue for the notion that intermediate metabolites (e.g., P5, 17-OHP4, and DHEA) are just leaked from the H295R cells into the media, whereas final products (probably 11-DOF, DHEA-S, and Δ5A-dione) are positively secreted from the H295R cells into the media.

5. Conclusions

The results imply the presence of combined steroidogenic characters of fetal adrenal and Leydig cells in this patient's c-ACC with a germline *TP53* mutation and several postzygotic carcinogenic events. However, the results have been obtained from a single c-ACC, and further studies are required to reveal steroidogenic and carcinogenic properties common to *TP53* mutation positive c-ACCs and those specific to each c-ACC.

Conflict of interest

The authors declare no conflict of interest.

Acknowledgments

We would like to thank Professor Hidenobu Sasano for the histopathological diagnosis.

This work was supported by Grants-in-Aid for Scientific Research on Innovative Areas from the Ministry of Education, Culture, Sports, Science and Technology (22132004-A01), by Grants-in-Aid for Scientific Research (A) from the Japan Society for the Promotion of Science (25253023), and by Grants for Research on Intractable Diseases from the Ministry of Health, Labor and Welfare (H27-025).

References

[1] R. Sandrini, R.C. Ribeiro, L. DeLacerda, Childhood adrenocortical tumors, J. Clin. Endocrinol. Metab. 82 (1997) 2027–2031.
[2] R.C. Ribeiro, F. Sandrini, B. Figueiredo, G.P. Zambetti, E. Michalkiewicz, A.R. Lafferty, L. DeLacerda, M. Rabin, C. Cadwell, G. Sampaio, I. Cat, C.A. Stratakis, R. Sandrini, An inherited p53 mutation that contributes in a tissue-specific manner to pediatric adrenal cortical carcinoma, Proc. Natl. Acad. Sci. U. S. A. 98 (2001) 9330–9335.
[3] E.M. Pinto, A.E. Billerbeck, M.C. Villares, S. Domenice, B.B. Mendonca, A.C. Latronico, Founder effect for the highly prevalent R337H mutation of tumor suppressor p53 in Brazilian patients with adrenocortical tumors, Arq. Bras. Endocrinol. Metab. 48 (2004) 647–650.
[4] S. Garritano, F. Gemignani, E.I. Palmero, M. Olivier, G. Martel-Planche, F. Le Calvez-Kelm, L. Brugieres, F.R. Vargas, R.R. Brentani, P. Ashton-Prolla, S. Landi, S.V. Tavtigian, P. Hainaut, M.I. Achatz, Detailed haplotype analysis at the TP53 locus in p.R337H mutation carriers in the population of Southern Brazil: evidence for a founder effect, Hum. Mutat. 31 (2010) 143–150.
[5] T. Else, A.C. Kim, A. Sabolch, V.M. Raymond, A. Kandathil, E.M. Caoili, S. Jolly, B. S. Miller, T.J. Giordano, G.D. Hammer, Adrenocortical carcinoma, Endocr. Rev. 35 (2014) 282–326.
[6] E. Letouze, R. Rosati, H. Komechen, M. Doghman, L. Marisa, C. Fluck, R.R. de Krijger, M.M. van Noesel, J.C. Mas, M.A. Pianovski, G.P. Zambetti, B.C. Figueiredo, E. Lalli, SNP array profiling of childhood adrenocortical tumors reveals distinct pathways of tumorigenesis and highlights candidate driver genes, J. Clin. Endocrinol. Metab. 97 (2012) E1284–1293.
[7] A.N. West, G.A. Neale, S. Pounds, B.C. Figueredo, C. Rodriguez Galindo, M.A. Pianovski, A.G. Oliveira Filho, D. Malkin, E. Lalli, R. Ribeiro, G.P. Zambetti, Gene expression profiling of childhood adrenocortical tumors, Cancer Res. 67 (2007) 600–608.
[8] L.F. Leal, L.M. Mermejo, L.Z. Ramalho, C.E. Martinelli Jr., J.A. Yunes, A.L. Seidinger, M.J. Mastellaro, I.A. Cardinalli, S.R. Brandalise, A.C. Moreira, L.G. Tone, C.A. Scrideli, M. Castro, S.R. Antonini, Wnt/beta-catenin pathway deregulation in childhood adrenocortical tumors, J. Clin. Endocrinol. Metab. 96 (2011) 3106–3114.
[9] C.L. Coulter, Fetal adrenal development: insight gained from adrenal tumors, Trends Endocrinol. Metab. 16 (2005) 235–242.
[10] E. Michalkiewicz, R. Sandrini, B. Figueiredo, E.C. Miranda, E. Caran, A.G. Oliveira-Filho, R. Marques, M.A. Pianovski, L. Lacerda, L.M. Cristofani, J. Jenkins, C. Rodriguez-Galindo, R.C. Ribeiro, Clinical and outcome characteristics of children with adrenocortical tumors: a report from the International Pediatric Adrenocortical Tumor Registry, J. Clin. Oncol. 22 (2004) 838–845.
[11] W. Bonfig, I. Bittmann, S. Bechtold, B. Kammer, V. Noelle, S. Arleth, K. Raile, H.P. Schwarz, Virilising adrenocortical tumours in children, Eur. J. Pediatr. 162 (2003) 623–628.
[12] S. Sbiera, S. Schmull, G. Assie, H.U. Voelker, L. Kraus, M. Beyer, B. Ragazzon, F. Beuschlein, H.S. Willenberg, S. Hahner, W. Saeger, J. Bertherat, B. Allolio, M. Fassnacht, High diagnostic and prognostic value of steroidogenic factor-1 expression in adrenal tumors, J. Clin. Endocrinol. Metab. 95 (2010) E161–171.
[13] N. Slade, U.M. Moll, Mutational analysis of p53 in human tumors: immunocytochemistry, Methods. Mol. Biol. 234 (2003) 231–243.
[14] A. Stojadinovic, M.F. Brennan, A. Hoos, A. Omeroglu, D.H. Leung, M.E. Dudas, A. Nissan, C. Cordon-Cardo, R.A. Ghossein, Adrenocortical adenoma and carcinoma: histopathological and molecular comparative analysis, Mod. Pathol. 16 (2003) 742–751.
[15] W.L. Miller, R.J. Auchus, The molecular biology biochemistry, and physiology of human steroidogenesis and its disorders, Endocr. Rev. 32 (2011) 81–151.
[16] L.M. Weiss, Comparative histologic study of 43 metastasizing and nonmetastasizing adrenocortical tumors, Am. J. Surg. Pathol. 8 (1984) 163–169.
[17] L.M. Weiss, L.J. Medeiros, A.L. Vickery Jr., Pathologic features of prognostic significance in adrenocortical carcinoma, Am. J. Surg. Pathol. 13 (1989) 202–206.
[18] S. Arai, Y. Shibata, Y. Nakamura, B. Kashiwagi, T. Uei, Y. Tomaru, Y. Miyashiro, S. Honma, K. Hashimoto, Y. Sekine, K. Ito, H. Sasano, K. Suzuki, Development of prostate cancer in a patient with primary hypogonadism: intratumoural steroidogenesis in prostate cancer tissues, Andrology 1 (2013) 169–174.
[19] M. Fukami, K. Homma, T. Hasegawa, T. Ogata, Backdoor pathway for dihydrotestosterone biosynthesis: implications for normal and abnormal human sex development, Dev. Dyn. 242 (2013) 320–329.
[20] C.C. Juhlin, G. Goh, J.M. Healy, A.L. Fonseca, U.I. Scholl, A. Stenman, J.W. Kunstman, T.C. Brown, J.D. Overton, S.M. Mane, C. Nelson-Williams, M. Backdahl, A.C. Suttorp, M. Haase, M. Choi, J. Schlessinger, D.L. Rimm, A. Hoog, M.L. Prasad, R. Korah, C. Larsson, R.P. Lifton, T. Carling, Whole-exome sequencing characterizes the landscape of somatic mutations and copy number alterations in adrenocortical carcinoma, J. Clin. Endocrinol. Metab. 100 (2015) E493–502.
[21] A.F. Gazdar, H.K. Oie, C.H. Shackleton, T.R. Chen, T.J. Triche, C.E. Myers, G.P. Chrousos, M.F. Brennan, C.A. Stein, R.V. La Rocca, Establishment and characterization of a human adrenocortical carcinoma cell line that expresses multiple pathways of steroid biosynthesis, Cancer Res. 50 (1990) 5488–5496.
[22] B. Staels, D.W. Hum, W.L. Miller, Regulation of steroidogenesis in NCI-H295 cells: a cellular model of the human fetal adrenal, Mol. Endocrinol. 7 (1993) 423–433.

[23] A. Ferlin, C. Foresta, Insulin-like factor 3: a novel circulating hormone of testicular origin in humans, Ann. N. Y. Acad. Sci. 1041 (2005) 497–505.
[24] E.E. Smeets, P.N. Span, A.E. van Herwaarden, R.A. Wevers, A.R. Hermus, F.C. Sweep, H.L. Claahsen-van der Grinten, Molecular characterization of testicular adrenal rest tumors in congenital adrenal hyperplasia: lesions with both adrenocortical and Leydig cell features, J. Clin. Endocrinol. Metab. 100 (2015) E524–530.
[25] M. Goto, K. Piper Hanley, J. Marcos, P.J. Wood, S. Wright, A.D. Postle, I.T. Cameron, J.I. Mason, D.I. Wilson, N.A. Hanley, In humans, early cortisol biosynthesis provides a mechanism to safeguard female sexual development, J. Clin. Invest. 116 (2006) 953–960.
[26] M. Katagiri, N. Kagawa, M.R. Waterman, The role of cytochrome b5 in the biosynthesis of androgens by human P450c17, Arch. Biochem. Biophys. 317 (1995) 343–347.
[27] V.A. Arboleda, H. Lee, R. Parnaik, A. Fleming, A. Banerjee, B. Ferraz-de-Souza, E. C. Delot, I.A. Rodriguez-Fernandez, D. Braslavsky, I. Bergada, E.C. Dell'Angelica, S.F. Nelson, J.A. Martinez-Agosto, J.C. Achermann, E. Vilain, Mutations in the PCNA-binding domain of CDKN1C cause IMAGe syndrome, Nat. Genet. 44 (2012) 788–792.
[28] R. Weksberg, C. Shuman, J.B. Beckwith, Beckwith-Wiedemann syndrome, Eur. J. Hum. Genet. 18 (2010) 8–14.
[29] F. Wilkin, N. Gagne, J. Paquette, L.L. Oligny, C. Deal, Pediatric adrenocortical tumors: molecular events leading to insulin-like growth factor II gene overexpression, J. Clin. Endocrinol. Metab. 85 (2000) 2048–2056.
[30] E. Samandari, P. Kempna, J.M. Nuoffer, G. Hofer, P.E. Mullis, C.E. Fluck, Human adrenal corticocarcinoma NCI-H295R cells produce more androgens than NCI-H295A cells and differ in 3beta-hydroxysteroid dehydrogenase type 2 and 17,20 lyase activities, J. Endocrinol. 195 (2007) 459–472.

EJHG Open

European Journal of Human Genetics (2015), 1–11
© 2015 Macmillan Publishers Limited All rights reserved 1018-4813/15
www.nature.com/ejhg

ARTICLE

Comprehensive clinical studies in 34 patients with molecularly defined UPD(14)pat and related conditions (Kagami–Ogata syndrome)

Masayo Kagami[1], Kenji Kurosawa[2], Osamu Miyazaki[3], Fumitoshi Ishino[4], Kentaro Matsuoka[5] and Tsutomu Ogata*[,1,6]

Paternal uniparental disomy 14 (UPD(14)pat) and epimutations and microdeletions affecting the maternally derived 14q32.2 imprinted region lead to a unique constellation of clinical features such as facial abnormalities, small bell-shaped thorax with a coat-hanger appearance of the ribs, abdominal wall defects, placentomegaly, and polyhydramnios. In this study, we performed comprehensive clinical studies in patients with UPD(14)pat ($n=23$), epimutations ($n=5$), and microdeletions ($n=6$), and revealed several notable findings. First, a unique facial appearance with full cheeks and a protruding philtrum and distinctive chest roentgenograms with increased coat-hanger angles to the ribs constituted the pathognomonic features from infancy through childhood. Second, birth size was well preserved, with a median birth length of ±0 SD (range, −1.7 to +3.0 SD) and a median birth weight of +2.3 SD (range, +0.1 to +8.8 SD). Third, developmental delay and/or intellectual disability was invariably present, with a median developmental/intellectual quotient of 55 (range, 29–70). Fourth, hepatoblastoma was identified in three infantile patients (8.8%), and histological examination in two patients showed a poorly differentiated embryonal hepatoblastoma with focal macrotrabecular lesions and well-differentiated hepatoblastoma, respectively. These findings suggest the necessity of an adequate support for developmental delay and periodical screening for hepatoblastoma in the affected patients, and some phenotypic overlap between UPD(14)pat and related conditions and Beckwith–Wiedemann syndrome. On the basis of our previous and present studies that have made a significant contribution to the clarification of underlying (epi)genetic factors and the definition of clinical findings, we propose the name 'Kagami–Ogata syndrome' for UPD(14)pat and related conditions.
European Journal of Human Genetics advance online publication, 18 February 2015; doi:10.1038/ejhg.2015.13

INTRODUCTION

Human chromosome 14q32.2 carries a cluster of imprinted genes including paternally expressed genes (*PEGs*) such as *DLK1* and *RTL1*, and maternally expressed genes (*MEGs*) such as *MEG3* (alias, *GTL2*), *RTL1as* (*RTL1* antisense), *MEG8*, *snoRNAs*, and *microRNAs* (Supplementary Figure S1).[1,2] The parental origin-dependent expression patterns are regulated by the germline-derived primary *DLK1-MEG3* intergenic differentially methylated region (IG-DMR) and the postfertilization-derived secondary *MEG3*-DMR.[2,3] Both DMRs are hypermethylated after paternal transmission and hypomethylated after maternal transmission in the body; in the placenta, the IG-DMR alone remains as a DMR with the same methylation pattern in the body, while the *MEG3*-DMR does not represent a differentially methylated pattern.[2,3] Consistent with such methylation patterns, the hypomethylated IG-DMR and *MEG3*-DMR of maternal origin function as imprinting control centers in the placenta and the body, respectively, and the IG-DMR behaves hierarchically as an upstream regulator for the methylation pattern of the *MEG3*-DMR in the body, but not in the placenta.[3,4]

Paternal uniparental disomy 14 (UPD(14)pat) (OMIM #608149) results in a unique constellation of clinical features such as facial abnormalities, small bell-shaped thorax with coat-hanger appearance of the ribs, abdominal wall defects, placentomegaly, and polyhydramnios.[2,5] These clinical features are also caused by epimutations (hypermethylations) and microdeletions affecting the maternally derived IG-DMR and/or *MEG3*-DMR (Supplementary Figure S1). Such UPD(14)pat and related conditions are rare, with reports of 33 patients with UPD(14)pat, five patients with epimutations, and nine patients with microdeletions (and four new UPD(14)pat patients reported here) (see Supplementary Table S1 for the reference list). For microdeletions, loss of the maternally inherited *MEG3*-DMR alone leads to a typical UPD(14)pat body phenotype and apparently normal placental phenotype,[3,4] whereas loss of the maternally derived IG-DMR alone or both DMRs results in a typical body and placental UPD(14)pat phenotype, consistent with the methylation patterns of the two DMRs.[2,3] Furthermore, correlations between clinical features and deleted segments have indicated the critical role of excessive *RTL1* (but not *DLK1*) expression in phenotypic development.[2,6] Such an excessive *RTL1* expression is primarily due to loss of functional *RTL1as*-encoded *microRNAs* that act as a *trans*-acting repressor for *RTL1* expression.[6] Indeed, the *RTL1* expression level is ~5 times, rather than 2 times, increased in placentas with UPD(14)pat

[1]Department of Molecular Endocrinology, National Research Institute for Child Health and Development, Tokyo, Japan; [2]Division of Medical Genetics, Kanagawa Children's Medical Center, Yokohama, Japan; [3]Department of Radiology, National Center for Child Health and Development, Tokyo, Japan; [4]Department of Epigenetics, Medical Research Institute, Tokyo Medical and Dental University, Tokyo, Japan; [5]Department of Pathology, National Center for Child Health and Development, Tokyo, Japan; [6]Department of Pediatrics, Hamamatsu University School of Medicine, Hamamatsu, Japan
*Correspondence: Dr T Ogata, Department of Pediatrics, Hamamatsu University School of Medicine, Hamamatsu 431-3192, Japan. Tel: +81 53 435 2310; Fax: +81 53 435 2310; E-mail: tomogata@hama-med.ac.jp
Received 30 August 2014; revised 7 January 2015; accepted 14 January 2015

Table 1 Clinical manifestations in 33 Japanese and one Irish patients with UPD(14)pat and related conditions (Kagami–Ogata syndrome)

	UPD(14)pat	*Epimutations*	*Microdeletions*				*Total*
			Subtype 1	*Subtype 2*	*Subtype 3*	*Subtotal*	
	Pts 1–23 (n = 23)	*Pts 24–28 (n = 5)*	*Pts 29–31 (n = 3)*	*Pt 32 (n = 1)*	*Pts 33–34 (n = 2)*	*Pts 29–34 (n = 6)*	*Pts 1–34 (n = 34)*
Age at the last examination or death (y)	2.9 (0.0–15.0)	2.0 (0.8–5.5)	2.8 (0.8–8.9)	(4 days)	4.5 (3.8–5.1)	3.3 (0.0–8.9)	2.8 (0.0–15.0)
Sex (male:female)	9:14	3:2	1:2	0:1	0:2	1:5	13:21
Molecular findings[a]							
IG-DMR of maternal origin	Absent	Methylated	Deleted	Unmethylated	Deleted		
MEG3-DMR of maternal origin	Absent	Methylated[b]	Deleted/methylated[b]	Deleted	Deleted		
DLK1 expression level	2×	2×	1 or 2×	2× (1×)[c]	1 or 2×		
RTL1 expression level	~5×	~5×	~5×	~5× (1× or ~2.5×)[c]	~2.5×		
MEGs expression level	0×	0×	0×	0× (1× or 0×)[c]	0×		
Pregnancy and delivery							
Polyhydramnios	23/23	5/5	3/3	0/1	2/2	5/6	33/34
Gestational age at Dx (w)	25 (14–30)	27.5 (22–30)	Unknown	—	21	21	25.5 (14–30)
Amnioreduction	18/20	4/5	2/3	0/1	1/2	3/6	25/31
Amnioreduction (>30 w)	18/18	4/4	2/2	—	1/1	3/3	25/25[d]
Placentomegaly[e]	14/17	4/4	3/3	0/1	2/2	5/6	23/27
Prenatal Dx of thoracic abnormality	8/20[f]	2/3	0/1	—	0/1	0/2	10/25
Gestational age at Dx (w)	26 (22–33)	27.5 (25–30)	—	—	—	—	26 (22–33)
Prenatal Dx of abdominal abnormality	6/18	3/3	1/1	—	0/1	1/2	10/23
Gestational age at Dx (w)	26 (22–28)	25	Unknown	Unknown	Unknown	Unknown	25.5 (22–28)
Gestational age (w)	34.5 (24–38)	35 (30–37)	30 (27–33)	28	32.5 (30–35)	30 (27–35)	34 (24–38)
Premature delivery (<37 w)	17/23	4/5	3/3	1/1	2/2	6/6	27/34
Delivery (Cesarean:Vaginal)	15:8	4:1	2:1	0:1	2:0	4:2	23:11
Medically assisted reproduction	1/18	0/1	0/1	Unknown	0/1	0/2	1/21
Growth pattern							
Prenatal growth failure[g]	0/23	0/5	0/3	0/1	0/2	0/6	0/34
Prenatal overgrowth[h]	13/23	3/5	3/3	0/1	1/2	4/6	20/34
Birth length (patient number)	21	5	1	1	2	4	30
SD score, median (range)	+0.3 (−1.7 to +3.0)	−0.5 (−0.9 to +1.4)	0.0	−1.1	+0.7 (−0.1 to +1.5)	−0.1 (−1.1 to +1.5)	±0 (−1.7 to +3.0)
Actual length (cm), median (range)	45.0 (30.6 to 51.0)	43.5 (41.0 to 50.0)	43.0	34.0	43.5 (42.0 to 45.0)	42.5 (34.0 to 45.0)	44.7 (30.6 to 51.0)
Birth weight (patient number)	23	5	3	1	2	6	34
SD score, median (range)	+2.2 (+0.1 +8.8)	+2.2 (+0.5 to +3.7)	+2.8 (+2.4 to +3.7)	+1.5	+1.7 (+0.9 to +2.5)	+2.5 (+0.9 to +3.7)	+2.3 (+0.1 to +8.8)
Actual weight (cm), median (range)	2.79 (1.24 to 3.77)	2.9 (1.61 to 3.28)	2.04 (1.30 to 2.84)	1.32	2.24 (1.55 to 2.94)	1.79 (1.30 to 2.94)	2.79 (1.24 to 3.77)
Postnatal growth failure[i]	7/20	2/5	2/3	—	0/2	2/5	11/30
Postnatal overgrowth[j]	1/20	1/5	0/3	—	0/2	0/5	2/30
Present stature (patient number)	20	5	3	—	1	4	29
SD score, median (range)	−1.6 (−8.7 to +1.1)	−1.8 (−7.1 to +0.9)	−2.2 (−3.3 to −1.3)	—	−1.6	−1.9 (−3.3 to −1.3)	−1.6 (−8.7 to +1.1)
Present weight (patient number)	20	5	3	—	2	5	30
SD score, median (range)	−1.0 (−6.0 to +2.4)	−0.6 (−5.5 to +4.0)	−1.3 (−2.2 to ±0)	—	−1.1 (−1.3 to −0.9)	−1.3 (−2.2 to ±0)	−1.0 (−6.0 to +4.0)

Table 1 (Continued)

	UPD(14)pat	Epimutations	Microdeletions				Total
			Subtype 1	Subtype 2	Subtype 3	Subtotal	
	Pts 1–23 (n = 23)	Pts 24–28 (n = 5)	Pts 29–31 (n = 3)	Pt 32 (n = 1)	Pts 33–34 (n = 2)	Pts 29–34 (n = 6)	Pts 1–34 (n = 34)
Craniofaciocervical features							
Frontal bossing	17/22	4/5	1/3	1/1	2/2	4/6	25/33
Hairy forehead	18/22	1/5	3/3	1/1	0/2	4/6	23/33
Blepharophimosis	18/22	3/5	2/3	0/1	1/2	3/6	24/33
Small ears	8/21	2/5	1/3	1/1	0/2	2/6	12/32
Depressed nasal bridge	23/23	5/5	3/3	0/1	1/2	4/6	32/34
Anteverted nares	19/22	4/5	3/3	0/1	2/2	5/6	28/33
Full cheek	20/21	4/4	2/2	0/1	1/1	3/4	27/29
Protruding philtrum	23/23	5/5	3/3	0/1	2/2	5/6	33/34
Puckered lips	11/21	3/5	3/3	0/1	0/2	3/6	17/32
Micrognathia	20/21	5/5	3/3	1/1	1/2	5/6	30/32
Short webbed neck	22/22	5/5	3/3	1/1	2/2	6/6	33/33
Thoracic abnormality							
Small bell-shaped thorax in infancy[k]	23/23	5/5	3/3	1/1	2/2	6/6	34/34
Coat-hanger appearance in infancy[l]	23/23	5/5	3/3	1/1	2/2	6/6	34/34
Laryngomalacia	8/20	2/5	2/3	—	0/1	2/4	12/29
Tracheostomy	7/21	1/4	0/2	—	2/2	2/4	10/29
Mechanical ventilation	21/23	5/5	3/3	1/1	2/2	6/6	32/34
Duration of ventilation (m)[m]	1.2 (0.1–17)	0.7 (0.1–0.9)	5 (0.23–10)	—	1.5 (1–2)	2 (0.2–10)	1.0 (0.1–17)
Abdominal wall defects							
Omphalocele	7/23	2/5	1/3	1/1	0/2	2/6	11/34
Diastasis recti	16/23	3/5	2/3	0/1	2/2	4/6	23/34
Developmental delay							
Developmental delay	21/21	5/5	3/3	—	2/2	5/5	31/31
Developmental/intellectual quotient	55 (29–70)	52 (48–56)	Unknown	Unknown	Unknown	—	55 (29–70)
Delayed head control (>4 m)[n]	14/16	4/4	1/1	—	1/1	2/2	20/22
Age at head control (m)[o]	7 (3–36)	7 (6–11)	6	—	6	6 (6)	7 (3–36)
Delayed sitting without support (>7 m)[n]	16/16	4/4	2/2	—	1/1	3/3	23/23
Age at sitting without support (m)[o]	12 (8–25)	11.5 (10–20)	22.5 (18–27)	—	18	18 (18–27)	12 (8–27)
Delayed walking without support (>14 m)[n]	17/17	3/3	2/2	—	2/2	4/4	24/24
Age at walking without support (m)[o]	25.5 (20–49)	25 (22–39)	60 (30–90)	—	24	30 (24–90)	25.5 (20–90)
Other features							
Feeding difficulty	20/21	5/5	3/3	—	2/2	5/5	30/31
Duration of tube feeding (m)[p]	6 (0.1–72)	8.5 (0.5–17)	59.5 (30–89)	—	51	51 (30–89)	7.5 (0.1–89)
Joint contractures	14/22	3/5	3/3	0/1	0/2	3/6	20/33
Constipation	12/20	3/4	1/2	—	0/2	1/4	16/28
Kyphoscoliosis	9/21	3/5	1/2	0/1	0/1	1/4	13/30

Table 1 (Continued)

	UPD(14)pat	*Epimutations*	*Microdeletions*				*Total*
			Subtype 1	*Subtype 2*	*Subtype 3*	*Subtotal*	
	Pts 1–23 (n = 23)	*Pts 24–28 (n = 5)*	*Pts 29–31 (n = 3)*	*Pt 32 (n = 1)*	*Pts 33–34 (n = 2)*	*Pts 29–34 (n = 6)*	*Pts 1–34 (n = 34)*
Coxa valga	6/21	1/5	3/3	0/1	1/2	4/6	11/32
Cardiac disease	5/22	1/5	0/3	1/1	1/2	2/6	8/33
Inguinal hernia	5/22	1/5	2/3	0/1	0/2	2/6	8/33
Seizure	1/21	0/5	0/3	0/1	0/2	0/6	1/32
Hepatoblastoma	3/23	0/5	0/3	0/1	0/2	0/6	3/34
Mortality within the first 5 years							
Alive:deceased	18:5	5:0	2:1	0:1	1:1	3:3	26:8
Parents							
Paternal age at childbirth (y)	35 (24–47)	30 (26–36)	37 (34–39)	25	31.5 (27–36)	35 (25–39)	34 (24–47)
Maternal age at childbirth (y)	31 (25–43)	28 (25–35)	31 (27–36)	25	30.5 (28–33)	29.5 (25–36)	31 (25–43)
Advanced childbearing age (⩾35 y)	8/23	1/5	1/3	0/1	0/2	1/6	8/34

Abbreviations: CHA, coat-hanger angle; Dx, diagnosis; m, month; M/W, mid to widest thorax diameter; UPD(14)pat, paternal uniparental disomy 14; w, week; y, year.
Patient #32 is Irish, and the remaining patients are Japanese; the Irish patient has also been examined by Beygo *et al*.[4]
Age data are expressed by median and range.
The denominators indicate the number of patients examined for the presence or absence of each feature, and the numerators represent the number of patient assessed to be positive for that feature; thus, differences between the denominators and numeratorsdenote the number of patients evaluated to be negative for the feature.
[a]For details, see Supplementary Figures S1 and S2.
[b]The *MEG3*-DMR is predicted to be grossly hypomethylated in the placenta.
[c]Expression patterns of the imprinted genes are predicted to be different between the body and the placenta in this patient, while they are predicted to be identical between the body and the placenta in other patients (See Supplementary Figure S1).
[d]Amnioreduction was performed about two times in 23 of the 25 pregnancies.
[e]Placental weight >120% of the gestational age-matched mean placental weight.[34]
[f]The diagnosis of UPD(14)pat has been suspected in two patients (patients #7 and #21).
[g]Birth length and/or birth weight <−2 SD of the gestational age- and sex-matched Japanese reference data (http://jspe.umin.jp/medical/keisan.html).
[h]Birth length and/or birth weight >+2 SD of the gestational age- and sex-matched Japanese reference data (http://jspe.umin.jp/medical/keisan.html).
[i]Present length/height and/or present weight <−2 SD of the age- and sex-matched Japanese reference data (http://jspe.umin.jp/medical/taikaku.html).
[j]Present length/height and/or present weight >+2 SD of the age- and sex-matched Japanese reference data (http://jspe.umin.jp/medical/taikaku.html).
[k]The M/W ratio below nromal range (see Figure 2).
[l]The CHA above the normal range (see Figure 2).
[m]The duration in patients in whom mechanical ventilation could be discontinued.
[n]The age when 90% of infants pass each gross motor developmental milestone (based on Revised Japanese Version of Denver Developmental Screening Test) (http://www.dinf.ne.jp/doc/japanese/prdl/jsrd/norma/n175/img/n175_078i01.gif).
[o]The median (range) of ages in patients who passed each gross motor developmental milestone; patients who have not passed each milestone are not included.
[p]The duration in patients in whom tube feeding could be discontinued.

accompanied by two copies of functional *RTL1* and no functional *RTL1as*.[6] This implies that the *RTL1* expression level is ~2.5 times increased in the absence of functional *RTL1as*-encoded *microRNAs*.

Here, we report comprehensive clinical findings in a series of patients with molecularly confirmed UPD(14)pat and related conditions, and suggest pathognomonic and/or characteristic features and their underlying factors. We also propose the name 'Kagami–Ogata syndrome' for UPD(14)pat and related conditions.

MATERIALS AND METHODS

Ethical approval

This study was approved by the Institute Review Board Committee at the National Center for Child Health and Development, and performed after obtaining written informed consent to publish the clinical and molecular information. We also obtained written informed consent with parental signature to publish facial photographs.

Patients

This study consisted of 33 Japanese patients and one Irish patient (patient #32) with UPD(14)pat and related conditions (13 males and 21 females; 31 patients with normal karyotypes and two patients (#17 and #20) with Robertsonian translocations involving chromosome 14 (karyotyping not performed in patient #1); 30 previously described patients[2,3,7–10] and four new patients) in whom underlying (epi)genetic causes were clarified and detailed clinical findings were obtained (Supplementary Table S2).

The 34 patients were classified into three groups according to the underlying (epi)genetic causes that were determined by methylation analysis for the two DMRs, microsatellite analysis for a total of 24 loci widely dispersed on chromosome 14, fluorescence *in situ* hybridization for the two DMRs, and oligonucleotide array-based comparative genomic hybridization for the 14q32.2 imprinted region, as reported previously:[9] (1) 23 patients with UPD(14)pat (UPD-group); (2) five patients with epimutations (Epi-group); and (3) six patients with microdeletions (Del-group) (Supplementary Figure S2).

Furthermore, the 23 patients of UPD-group were divided into three subtypes in terms of UPD generation mechanisms by microsatellite analysis, as reported previously:[9] (1) 13 patients with monosomy rescue (MR) or postfertilization mitotic error (PE)-mediated UPD(14)pat indicated by full isodisomy (subtype 1) (UPD-S1); (2) a single patient with PE-mediated UPD(14)pat demonstrated by segmental isodisomy (subtype 2) (UPD-S2); and (3) nine patients with trisomy rescue (TR) or gamete complementation (GC)-mediated UPD(14)pat revealed by heterodisomy for at least one locus (subtype 3) (UPD-S3) (Supplementary Figure S2) (it is possible that some patients classified as UPD-S1 may have a cryptic heterodisomic region(s) and actually belong to UPD-S3). Similarly, the six patients of Del-group were divided into three subtypes in terms of the measured/predicted *RTL1* expression level in the body and placenta:[2,3] (1) three patients with ~5 times *RTL1* expression level in both the body and placenta (subtype 1) (Del-S1); (2) a single patient with about five times *RTL1* expression level in the body and normal (1 time) or ~2.5 times *RTL1* expression level in the placenta (subtype 2) (Del-S2); and (3) two patients with ~2.5 times *RTL1* expression level in both the body and placenta (subtype 3) (Del-S3) (Supplementary Figure S2). The measured/predicted expression patterns of the imprinted genes in each group/subtype are illustrated in Supplementary Figure S1.

Clinical studies

We used a comprehensive questionnaire to collect detailed clinical data of all patients from attending physicians. To evaluate chest roentgenographic findings, we obtained the coat-hanger angle (CHA) to the ribs and the ratio of the mid to widest thorax diameter (M/W ratio), as reported previously.[11] We also asked the physicians to report any clinical findings not covered by the questionnaire.

Statistical analysis

Statistical significance of the median among three groups and between two groups/subtypes was examined by the Kruskal–Wallis test and the Mann–Whitney's *U*-test, respectively, and that of the frequency among three groups and between two groups was analyzed by the Fisher's exact probability test, using the R environment (http://cran.r-project.org/bin/windows/base/old/2.15.1/). $P<0.05$ was considered significant. Kaplan–Meier survival curves were constructed using the R environment.

RESULTS

Clinical findings of each group/subtype are summarized in Table 1, and those of each patient are shown in Supplementary Table S2. Phenotypic findings were comparable among UPD-S1, UPD-S2, and UPD-S3, and somewhat different among Del-S1, Del-S2, and Del-S3, as predicted from the expression patterns of the imprinted genes (Supplementary Figure S1). Thus, we showed the data of UPD-group (the sum of UPD-S1, UPD-S2, and UPD-S3) and those of each subtype of Del-group (Del-S1, Del-S2, and Del-S3) in Table 1, and described the data of UPD-S1, UPD-S2, and UPD-S3 in Supplementary Table S3.

We registered the clinical information of each patient in the Leiden Open Variation Database (LOVD) (http://www.lovd.nl/3.0/home; http://databases.lovd.nl/shared/individuals), and the details of each microdeletion in the ClinVar Database (http://www.ncbi.nlm.nih.gov/clinvar/). The LOVD Individual IDs and the ClinVar SCV accession numbers are shown in Supplementary Table S2.

Pregnancy and delivery

Polyhydramnios was observed from ~25 weeks of gestation during the pregnancies of all patients, except for patient #32 of Del-S2 who had deletion of the *MEG3*-DMR and three of the seven *MEG3* exons, and usually required repeated amnioreduction, especially after 30 weeks of gestation. Placentomegaly was usually identified in patients affected with polyhydramnios, but not found in three patients of UPD-group. Thoracic and abdominal abnormalities were found by ultrasound studies in ~40% of patients from ~25 weeks of gestation, and UPD(14)pat was suspected in patients #7 and #21, due to delineation of the bell-shaped thorax with coat-hanger appearance of the ribs. Premature delivery was frequently observed, especially in Del-group. Because of fetal distress and polyhydramnios, ⩾two-thirds of the patients in each group were delivered by Cesarean section. Medically assisted reproduction was reported only in one (patient #8) of 21 patients for whom clinical records on conception were available.

Growth pattern

Prenatal growth was characterized by grossly normal birth length and obviously excessive birth weight. Indeed, birth length ranged from 30.6 to 51.0 cm (−1.7 to +3.0 SD for the gestational age- and sex-matched Japanese reference data) with a median of 44.7 cm (±0 SD), and birth weight ranged from 1.24 to 3.77 kg (+0.1 to +8.8 SD) with a median of 2.79 kg (+2.3 SD). Although birth weight was disproportionately greater than birth length, there was no generalized edema as a possible cause of overweight.

In contrast, postnatal growth was rather compromised, and growth failure (present length/height and/or weight < -2 SD) was observed in about one-third of patients of each group. Postnatal weight was better preserved than postnatal length/height.

Craniofaciocervical features

All patients exhibited strikingly similar craniofaciocervical features (Figure 1). Indeed, >90% of patients had depressed nasal bridge, full cheeks, protruding philtrum, micrognathia, and short webbed neck. In particular, the facial features with full cheeks and protruding philtrum

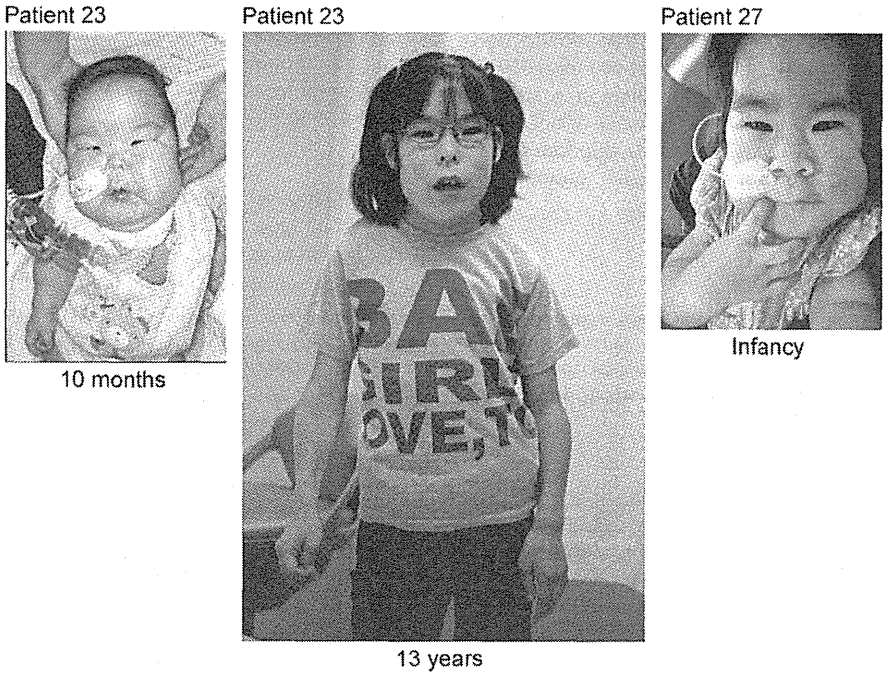

Figure 1 Photographs of patient #23 with UPD(14)pat and patient #27 with epimutation.

appeared to be specific to UPD(14)pat and related conditions, and were recognizable from infancy through childhood.

Thoracic abnormality

The 34 patients invariably showed small bell-shaped small thorax with coat-hanger appearance of the ribs in infancy (Figure 2). Long-term (≥10 years) follow-up in patient #12 of UPD-group and patient #31 of Del-S1 who had ~5 times of *RTL1* expression, and in patient #34 of Del-S3 who had ~2.5 times of *RTL1* expression, showed that the CHAs remained above the normal range of age-matched control children, while the M/W ratios, though they were below the normal range in infancy, became within the normal range after infancy (Figure 2). Laryngomalacia was also often detected in each group.

Mechanical ventilation was performed in all patients except for patients #14 and #20 of UPD-group, and tracheostomy was also carried out in about one-third of patients. Mechanical ventilation could be discontinued during infancy in 22 patients (Supplementary Figure S3). Ventilation duration was variable with a median period of 1 month among the 22 patients, and was apparently unrelated to the underlying genetic cause or gestational age.

Abdominal wall defects

Omphalocele was identified in about one-third of patients, and diastasis recti was found in the remaining patients.

Developmental status

Developmental delay (DD) and/or intellectual disability (ID) was invariably present in 26 patients examined (age, 10 months to 15 years), with the median developmental/intellectual quotient (DQ/IQ) of 55 (range, 29–70) (Figure 3). Gross motor development was also almost invariably delayed, with grossly similar patterns among different groups. In patients who passed gross motor developmental milestones, head control was achieved at ~7 months, sitting without support at ~12 months, and walking without support at ~2.1 years of age.

Other features

Several prevalent features were also identified. In particular, except for patient #22, feeding difficulty with poor sucking and swallowing was exhibited by all patients who were affected with polyhydramnios, and gastric tube feeding was performed in all patients who survived more than 1 week (Supplementary Figure S4). Tube-feeding duration was variable with a median period of ~7.5 months in 16 patients for whom tube feeding was discontinued, and tended to be longer in Del-group. In addition, there were several features manifested by single patients (Supplementary Table S2).

Notably, hepatoblastoma was identified at 46 days of age in patient #17, at 218 days in patient #18, and at 13 months of age in patient #8 of UPD-group (Figure 4). It was surgically removed in patients #8 and #18, although chemotherapy was not performed because of poor body condition. In patient #17, neither an operation nor chemotherapy could be carried out because of the patient's severely poor body condition. Histological examination of the removed tumors revealed a poorly differentiated embryonal hepatoblastoma with focal macrotrabecular lesions in patient #8 (Figure 4) and a well-differentiated hepatoblastoma in patient #18.[10]

Mortality

Eight patients were deceased before 4 years of age. The survival rate was 78% in UPD-group, 100% in Epi-group, and 50% in Del-group; it was 25% in patients born ≤29 weeks of gestation, 83% in those born 30–36 weeks of gestation, and 86% in those born ≥37 weeks of gestation (Figure 5). The cause of death was variable; however, respiratory problems were a major factor, because patient #1 died

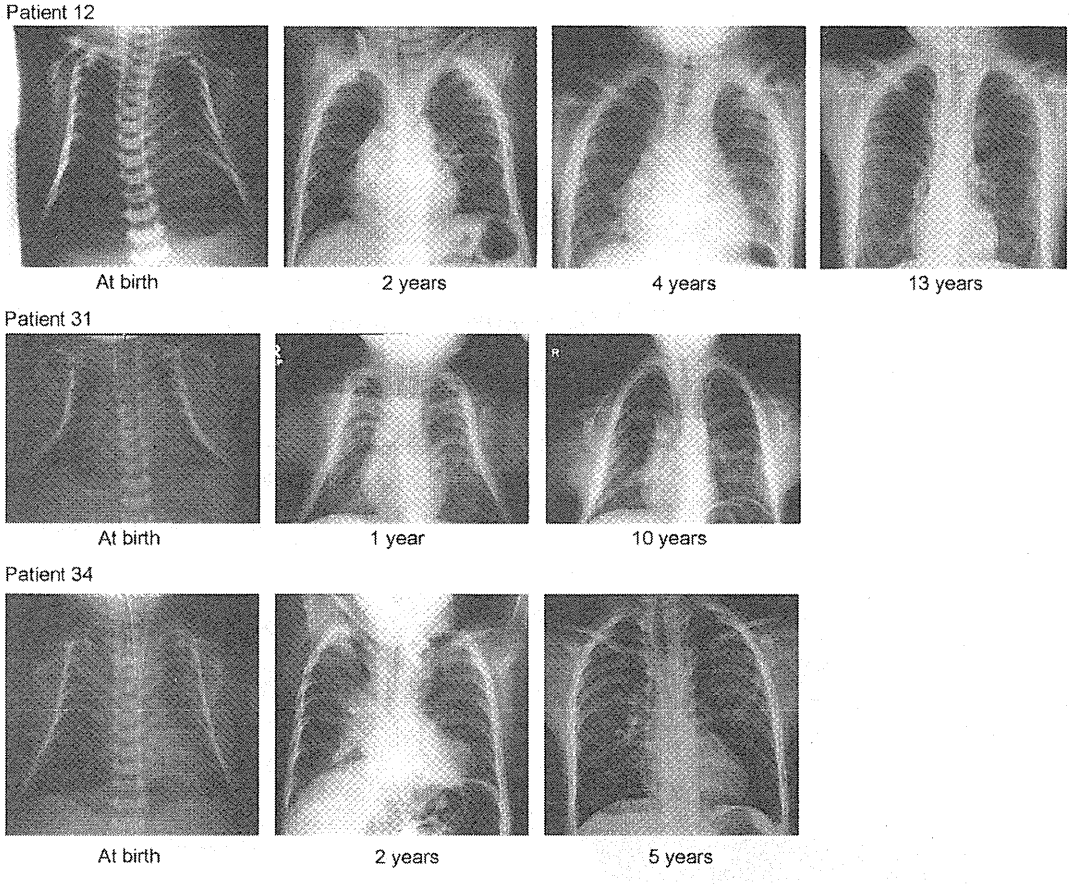

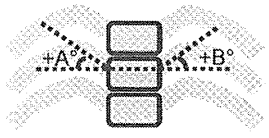

CHA = (A + B) ÷ 2
(6th posterior ribs)

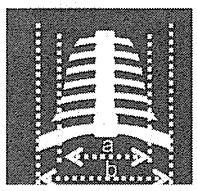

M/W ratio = a / b

		CHA	M/W ratio	
Patient 12	At birth	41	70	
	2 years	39	88	
	4 years	42	94	
	13 years	39	92	
Patient 31	At birth	35	58	
	1 year	28	80	
	10 years	29	85	
Patient 34	At birth	44	70	
	2 year	48	93	
	5 years	37	96	
UPD(14)pat	At birth	+28 ~ +45	58 ~ 80	(n=8)
	~ 5 years	+25 ~ +45	>78%	(n=3)
Controls	At birth	–11 ~ +1.9	82 ~ 89	(n=10)
	~ 5 years	–21 ~ +15	83 ~ 98	(n=10)
	~ 10 years	–9.3 ~ +20	91 ~ 100	(n=10)

Figure 2 Chest roentgenograms of patient #12 of UPD-group, patient #31 of Del-S1, and patient #34 of Del-S3. *RTL1* expression level is predicted to be ~5 times higher in patients #12 and #31, and ~2.5 times higher in patient #34. The CHA to the ribs remains above the normal range throughout the study period, whereas the M/W ratio (the ratio of the mid to widest thorax diameter) normalizes with age.

of neonatal respiratory distress syndrome, and patients #8, #30 and #33 died during a respiratory infection. Of the three patients with hepatoblastoma, patient #17 died of hepatoblastoma, whereas patient #8 died during influenza infection and patient #18 died of hemophagocytic syndrome.

Comparison among/between different groups/subtypes

Clinical findings were grossly similar among/between different groups/subtypes with different expression dosages of *RTL1* and *DLK1*. However, significant differences were found for short gestational age and long duration of tube feeding in Del-group (among three groups

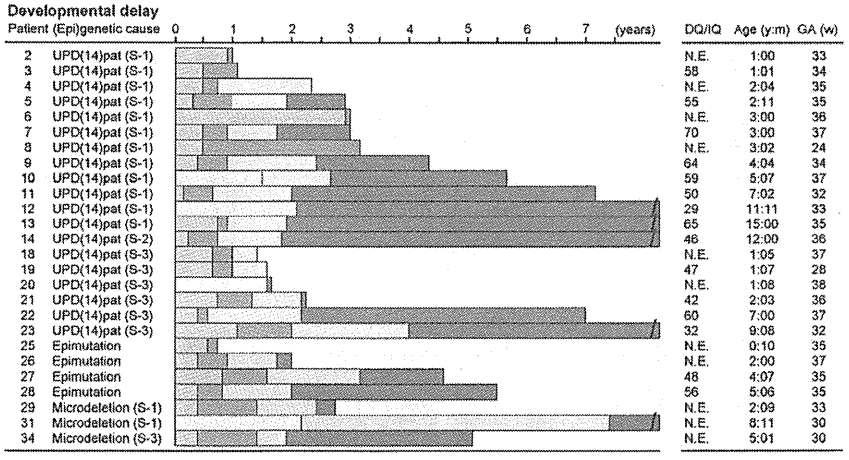

Figure 3 Developmental status. The orange, green, yellow, and blue bars represent the period before head control, the period after head control and before sitting without support, the period after sitting without support and before walking without support, and the period after walking without support, respectively. The gray bars denote the period with no information. DQ, developmental quotient; IQ, intellectual quotient; N.E., not examined; Age, age at the last examination or at death; and GA, gestational age.

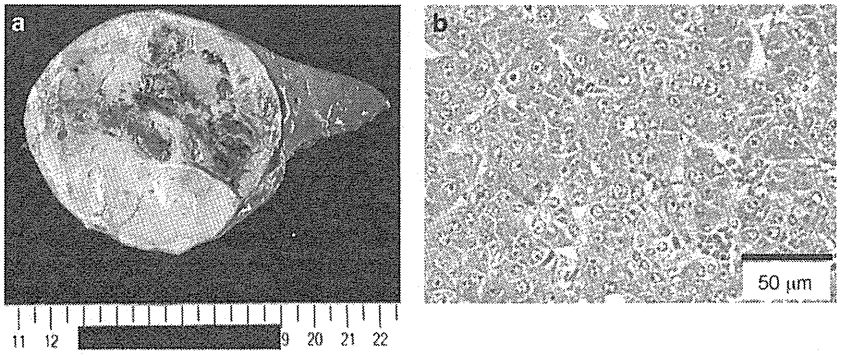

Figure 4 Hepatoblastoma in patient #8 of UPD-group. **(a)** Macroscopic appearance of the hepatoblastoma with a diameter of ~8 cm. **(b)** Microscopic appearance of the hepatoblastoma exhibiting a trabecular pattern. The hepatoblastoma cells are associated with eosinophilic cytoplasm and large nuclei, and resemble fetal hepatocytes.

and against Epi-group and UPD-group) and infrequent hairy forehead in Epi-group (among three groups and against UPD-group) (actual *P*-values are available on request).

DISCUSSION

We examined detailed clinical findings in patients with UPD(14)pat and related conditions. The results indicate that the facial features with full cheeks and protruding philtrum and the thoracic roentgenographic findings with increased CHAs to the ribs represent the pathognomonic features of UPD(14)pat and related conditions from infancy through the childhood. In addition, the decreased M/W ratios also denote the diagnostic hallmark in infancy, but not after infancy. Although other features such as polyhydramnios, placentomegaly, and abdominal wall defects are characteristic of UPD(14)pat and related conditions, they would be regarded as rather nonspecific features that are also observed in other conditions such as Beckwith–Wiedemann syndrome (BWS) (Supplementary Table S4).[12,13]

Such body and placental features were similarly exhibited by patients of each group/subtype, including those of Del-S1, Del-S2, and Del-S3 with different expression dosage of *DLK1* (1× or 2×) and *RTL1* (~2.5× or ~5×), except for patient #32 of Del-S2 who showed typical body features but apparently lacked placental features. Indeed, the difference in the *DLK1* expression dosage had no discernible clinical effects, although mouse *Dlk1* is expressed in several fetal tissues, including the ribs.[14,15] Similarly, in contrast to our previous report which suggested a possible dosage effect of *RTL1* expression level on the phenotypic severity,[2] the difference in the *RTL1* expression dosage turned out to have no recognizable clinical effects after analyzing long-term clinical courses in the affected patients. This suggests that ~2.5×*RTL1* expression is the primary factor for the phenotypic development in the body and placenta. Consistent with the critical role of excessive *RTL1* expression in the phenotypic development, mouse *Rtl1* is clearly expressed in the fetal ribs and skeletal muscles (Supplementary Figure S5) as well as in the placenta,[16,17] and human *RTL1* mRNA and RTL1 protein are strongly expressed in placentas with UPD(14)pat.[6] Thus, lack of placental abnormalities in patient #32 can be explained by assuming a positive *RTL1as* expression and resultant normal (1×) *RTL1* expression in the placenta (Supplementary Figure S1). In addition, since mouse *Gtl2* (*Meg3*) is expressed in multiple fetal tissues including the primordial cartilage,[14] this may argue for the positive role of absent *MEGs* expression in phenotypic development.

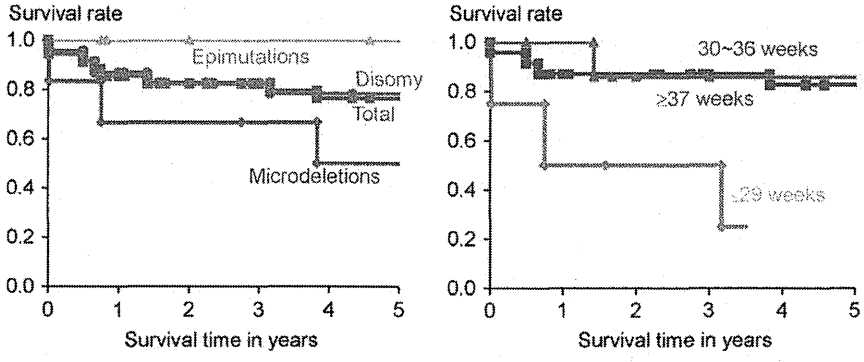

Patient	(Epi)genetic cause	GA	Cause of death	Age of death
1	UPD(14)pat (S-1)	34	Respiratory failure	2 hours
8	UPD(14)pat (S-1)	24	Influenza infection	3 2/12 yrs
15	UPD(14)pat (S-3)	34	Necrotizing enterocolitis	6 mos
17	UPD(14)pat (S-3)	32	Hepatoblastoma	8 mos
18	UPD(14)pat (S-3)	37	Hemophagocytic syndrome	1 5/12 yrs
30	Microdeletion (S-1)	27	Sudden death at URI	9 mos
32	Microdeletion (S-2)	28	Intracranial hemorrhage	4 days
33	Microdeletion (S-3)	35	RS virus infection	3 10/12 yrs

Figure 5 Kaplan–Meier survival curves according to the (epi)genetic cause and the gestational age (week), and summary of the causes of death. GA, gestational age; URI, upper respiratory infection; and RS, respiratory syncytial. Patients #8, #17, and #18 had hepatoblastoma.

The present study revealed several notable findings. First, polyhydramnios was identified during the pregnancies of nearly all patients, except for patient #32 of Del-S2. Amniotic fluid originates primarily from fetal urine and is absorpted primarily by fetal swallowing into the digestive system.[18,19] Since fetal hydration and the resultant urine flow mainly depend on the water flow from maternal circulation across the placenta,[19] placentomegaly would have facilitated the production of amniotic fluid. Furthermore, since feeding difficulty with impaired swallowing was observed in most patients, defective swallowing would have compromised absorption of amniotic fluid. Thus, both body and placental factors are assumed for the development of polyhydramnios. This would explain why polyhydramnios was observed in patients #1, #6, and #8 who were free from placentomegaly, and in patient #22 who showed no feeding difficulty, although the presence of feeding difficulty was unknown for patient #1 as was placentomegaly for patient #22. In addition, since amniotic fluid begins to increase from 8–11 weeks of gestation and reaches its maximum volume around 32 weeks of gestation,[18,19] this would explain why amnioreduction was usually required from 30 weeks of gestation.

Second, birth size was relatively well preserved, whereas postnatal growth was rather compromised. The well preserved prenatal growth in apparently compromised intrauterine environments would be consistent with the conflict theory that overexpression of *PEGs* promotes fetal and placental growth.[20] Notably, birth weight was disproportionately greater than birth length in the apparent absence of generalized edema. In this regard, mouse *Dlk1*, *Rtl1*, and *Gtl2* (*Meg3*) on the distal part of chromosome 12 are expressed in skeletal muscles (Supplementary Figure S5),[14,17] and paternal disomy for chromosome 12 causes muscular hypertrophy.[21] Thus, patients with UPD(14)pat and related conditions may have muscular hypertrophy especially in the fetal life. The compromised postnatal growth would primarily be because of poor nutrition caused by feeding difficulties, whereas relative overweight suggestive of possible muscular hypertrophy remains to be recognized.

Third, DD/ID was invariably present in all 26 patients examined for their developmental/intellectual status, with the median DQ/IQ of 55. In this regard, mouse *Dlk1*, *Rtl1*, and *Gtl2* (*Meg3*) are expressed in the brain during embryogenesis (Supplementary Figure S5),[22] and *Dlk1* is involved in the differentiation of midbrain dopaminergic neurons.[22] Thus, DD/ID would primarily be ascribed to the altered expression dosage of *PEGs/MEGs* in the brain.

Fourth, hepatoblastoma was identified in three patients of UPD-group during infancy. In this context, it has been reported that (1) mouse *Dlk1*, *Rtl1*, and *Meg3* (*Gtl2*) are expressed in the fetal liver, but not in the adult liver; [14,17,23,24] (2) overexpression of *Rtl1* in the adult mouse liver has induced hepatic tumors with high penetrance;[24] (3) *Meg3* functions as a tumor suppressor gene in mice;[25] (4) human *DLK1* is expressed in the hepatocytes of 5–6 weeks old embryos;[26] and (5) human DLK1 protein is upregulated in hepatoblastoma.[27] These findings imply the relevance of excessive *RTL1* expression and loss of *MEG3* expression to the occurrence of hepatoblastoma in UPD(14)pat and related conditions, while it remains to be determined whether the DLK1 upregulation is the cause or the result of hepatoblastoma development. Thus, periodical screening for hepatoblastoma, such as serum α-fetoprotein measurement and abdominal ultrasonography, is recommended. In this context, it remains to be studied whether other embryonal tumors may also be prone to occur in UPD(14)pat and related conditions.

Fifth, mortality was high in Del-group and null in Epi-group. The high mortality in Del-group would primarily be ascribed to the high prevalence of premature delivery, although it is unknown whether the high prevalence of premature delivery is an incidental finding or characteristic of Del-group. The null mortality in Epi-group may be due to possible mosaicism with cells accompanied by a normal expression pattern because of escape from epimutation, as reported previously.[28,29] It is unknown, however, whether possible presence of trisomic cells in TR-mediated UPD(14)pat and that of normal cells in PE-mediated UPD(14) may have exerted clinical effects. Notably, since

death was observed only in patients <4 years of age, the vital prognosis is expected to be good from childhood. In addition, since three patients died during respiratory infections, careful management is recommended during such infections.

Furthermore, the present study also provides several useful clinical implications: (1) two patients had Robertsonian translocations as a risk factor for the development of UPD.[30] Thus, karyotyping is suggested for patients with an UPD(14)pat-like phenotype; (2) prenatal detection of polyhydramnios and thoracic and abdominal features is possible from ~25 weeks of gestation; (3) mechanical ventilation and gastric tube feeding are usually required, with variable durations; (4) there was no patient in UPD-group who exhibited clinical features that are attributable to the unmasking of a recessive mutation(s) of paternal origin; (5) since UPD(14)pat and related conditions share several clinical features including embryonal tumors with BWS (Supplementary Table S4), UPD(14)pat and related conditions may be worth considering in atypical or underlying factor-unknown BWS; and (6) since clinical findings are comparable between patients examined in this study and 17 similarly affected non-Japanese patients (Supplementary Table S5), our data will be applicable to non-Japanese patients as well.

A critical matter for UPD(14)pat and related conditions is the lack of a syndrome name. Although the term 'UPD(14)pat syndrome' has been utilized previously,[4] the term is confusing because 'UPD(14)pat syndrome' can be caused by (epi)genetic mechanisms other than UPD (14)pat. In this regard, the name 'Temple syndrome' has been proposed for UPD(14)mat and related conditions or 'UPD(14)mat syndrome',[31,32] a mirror image of UPD(14)pat and related conditions. On the basis of our previous and present studies that have made a significant contribution to the clarification of underlying (epi)genetic factors and the definition of clinical findings, we would propose the name 'Kagami–Ogata syndrome', or 'Wang–Kagami–Ogata syndrome' with the name of Wang who first described UPD(14)pat,[33] for UPD (14)pat and related conditions.

In summary, although the number of patients still remains small, especially in each subtype of Del-group, the present study reveals pathognomic and characteristic clinical findings in UPD(14)pat and related conditions. Furthermore, this study shows the invariable occurrence of DD/ID and the occasional (8.8%) development of hepatoblastoma, thereby showing the necessity of adequate support for DD/ID and screening of hepatoblastoma in affected patients. Finally, we propose the name 'Kagami–Ogata syndrome' for UPD(14)pat and related conditions.

CONFLICT OF INTEREST

The authors declare no conflict of interest.

ACKNOWLEDGEMENTS

We are grateful to all patients and their parents for their cooperation. We thank Drs Haruhiko Sago, Aiko Sasaki, Jun Shibasaki, Rika Kosaki, Michiko Hayashidani, Toshio Takeuchi, Shinya Tanaka, Mika Noguchi, Goro Sasaki, Kouji Matsumoto, Takeshi Utsunomiya, Yumiko Komatsu, Hirofumi Ohashi, Hiroshi Kishimoto, Maureen J O'Sullivan, Andrew J Green, Yoshiyuki Watabe, Tsuyako Iwai, Hitoshi Kawato, Akiko Yamamoto, Nobuhiro Suzumori, Hiroko Ueda, Makoto Kuwajima, Kiyoko Samejima, Hiroshi Yoshihashi, Yoriko Watanabe, Jin Nishimura, Shuku Ishikawa, Michiko Yamanaka, Machiko Nakagawa, Hiroharu Inoue, Takashi Imamura, Keiichi Motoyama and Ryoko Yoshinare for providing us with detailed clinical data and materials for molecular studies, Dr Gen Nishimura for interpretation of roentgengraphic findings, and Drs Tadayuki Ayabe, Keiko Matsubara, Yoichi Sekita and Maki Fukami for their support in molecular analyses. We also thank Ms. Emma Barber for her editorial assistance with the final draft of this paper. This work was supported by: Grants-in-Aid for Scientific Research (A) (25253023) and Research (B) (23390083) from the Japan Society for the Promotion of Science (JSPS), and by Grants for Health Research on Children, Youth, and Families (H25-001) and for Research on Intractable Diseases (H22-161) from the Ministry of Health, Labor and Welfare (MHLW), by Grants from the National Center for Child Health and Development (23A-1, 25-10), and by a Grant from Takeda Science Foundation.

1 da Rocha ST, Edwards CA, Ito M, Ogata T, Ferguson-Smith AC: Genomic imprinting at the mammalian Dlk1-Dio3 domain. *Trends Genet* 2008; **24**: 306–316.
2 Kagami M, Sekita Y, Nishimura G *et al*: Deletions and epimutations affecting the human 14q32.2 imprinted region in individuals with paternal and maternal upd(14)-like phenotypes. *Nat Genet* 2008; **40**: 237–242.
3 Kagami M, O'Sullivan MJ, Green AJ *et al*: The IG-DMR and the MEG3-DMR at human chromosome 14q32.2: hierarchical interaction and distinct functional properties as imprinting control centers. *PLoS Genet* 2010; **6**: e1000992.
4 Beygo J, Elbracht M, de Groot K *et al*: Novel deletions affecting the MEG3-DMR provide further evidence for a hierarchical regulation of imprinting in 14q32. *Eur J Hum Genet* 2015; **23**: 180–188.
5 Hoffmann K, Heller R: Uniparental disomies 7 and 14. *Best Pract Res Clin Endocrinol Metab* 2011; **25**: 77–100.
6 Kagami M, Matsuoka K, Nagai T *et al*: Paternal uniparental disomy 14 and related disorders: placental gene expression analyses and histological examinations. *Epigenetics* 2012; **7**: 1142–1150.
7 Kurosawa K, Sasaki H, Sato Y *et al*: Paternal UPD14 is responsible for a distinctive malformation complex. *Am J Med Genet* 2002; **110**: 268–272.
8 Kagami M, Nishimura G, Okuyama T *et al*: Segmental and full paternal isodisomy for chromosome 14 in three patients: narrowing the critical region and implication for the clinical features. *Am J Med Genet A* 2005; **138A**: 127–132.
9 Kagami M, Kato F, Matsubara K, Sato T, Nishimura G, Ogata T: Relative frequency of underlying genetic causes for the development of UPD(14)pat-like phenotype. *Eur J Hum Genet* 2012; **20**: 928–932.
10 Horii M, Horiuchi H, Momoeda M, Nakagawa M *et al*: Hepatoblastoma in an infant with paternal uniparental disomy 14. *Congenit Anom (Kyoto)* 2012; **52**: 219–220.
11 Miyazaki O, Nishimura G, Kagami M, Ogata T: Radiological evaluation of dysmorphic thorax of paternal uniparental disomy 14. *Pediatr Radiol* 2011; **41**: 1013–1019.
12 Parveen Z, Tongson-Ignacio JE, Fraser CR, Killeen JL, Thompson KS: Placental mesenchymal dysplasia. *Arch Pathol Lab Med* 2007; **131**: 131–137.
13 Williams DH, Gauthier DW, Maizels M: Prenatal diagnosis of Beckwith–Wiedemann syndrome. *Prenat Diagn* 2005; **25**: 879–884.
14 da Rocha ST, Tevendale M, Knowles E, Takada S, Watkins M, Ferguson-Smith AC: Restricted co-expression of Dlk1 and the reciprocally imprinted non-coding RNA, Gtl2: implications for cis-acting control. *Dev Biol* 2007; **306**: 810–823.
15 da Rocha ST, Charalambous M, Lin SP *et al*: Gene dosage effects of the imprinted delta-like homologue 1 (dlk1/pref1) in development: implications for the evolution of imprinting. *PLoS Genet* 2009; **5**: e1000392.
16 Sekita Y, Wagatsuma H, Nakamura K *et al*: Role of retrotransposon-derived imprinted gene, Rtl1, in the feto-maternal interface of mouse placenta. *Nat Genet* 2008; **40**: 243–248.
17 Brandt J, Schrauth S, Veith AM *et al*: Transposable elements as a source of genetic innovation: expression and evolution of a family of retrotransposon-derived neogenes in mammals. *Gene* 2005; **345**: 101–111.
18 Modena AB, Fieni S: Amniotic fluid dynamics. *Acta Biomed* 2004; **75**: 11–13.
19 Beall MH, van den Wijngaard JP, van Gemert MJ, Ross MG: Amniotic fluid water dynamics. *Placenta* 2007; **28**: 816–823.
20 Hurst LD, McVean GT: Growth effects of uniparental disomies and the conflict theory of genomic imprinting. *Trends Genet* 1997; **13**: 436–443.
21 Georgiades P, Watkins M, Surani MA, Ferguson-Smith AC: Parental origin-specific developmental defects in mice with uniparental disomy for chromosome 12. *Development* 2000; **127**: 4719–4728.
22 Wilkinson LS, Davies W, Isles AR: Genomic imprinting effects on brain development and function. *Nat Rev Neurosci* 2007; **8**: 832–843.
23 Kang ER, Iqbal K, Tran DA *et al*: Effects of endocrine disruptors on imprinted gene expression in the mouse embryo. *Epigenetics* 2011; **6**: 937–950.
24 Riordan JD, Keng VW, Tschida BR *et al*: Identification of rtl1, a retrotransposon-derived imprinted gene, as a novel driver of hepatocarcinogenesis. *PLoS Genet* 2013; **9**: e1003441.
25 Zhou Y, Zhang X, Klibanski A: MEG3 noncoding RNA: a tumor suppressor. *J Mol Endocrinol* 2012; **48**: R45–R53.
26 Floridon C, Jensen CH, Thorsen P *et al*: Does fetal antigen 1 (FA1) identify cells with regenerative, endocrine and neuroendocrine potentials? A study of FA1 in embryonic, fetal, and placental tissue and in maternal circulation. *Differentiation* 2000; **66**: 49–59.
27 Falix FA, Aronson DC, Lamers WH, Hiralall JK, Seppen J: DLK1, a serum marker for hepatoblastoma in young infants. *Pediatr Blood Cancer* 2012; **59**: 743–745.
28 Yamazawa K, Kagami M, Fukami M, Matsubara K, Ogata T: Monozygotic female twins discordant for Silver-Russell syndrome and hypomethylation of the H19-DMR. *J Hum Genet* 2008; **53**: 950–955.

29 Azzi S, Blaise A, Steunou V *et al*: Complex tissue-specific epigenotypes in Russell–Silver Syndrome associated with 11p15 ICR1 hypomethylation. *Hum Mutat* 2014; **35**: 1211–1220.
30 Berend SA, Horwitz J, McCaskill C, Shaffer LG: Identification of uniparental disomy following prenatal detection of Robertsonian translocations and isochromosomes. *Am J Hum Genet* 2000; **66**: 1787–1793.
31 Ioannides Y, Lokulo-Sodipe K, Mackay DJ, Davies JH, Temple IK: Temple syndrome: improving the recognition of an underdiagnosed chromosome 14 imprinting disorder: an analysis of 51 published cases. *J Med Genet* 2014; **51**: 495–501.
32 Hosoki K, Kagami M, Tanaka T *et al*: Maternal uniparental disomy 14 syndrome demonstrates Prader–Willi syndrome-like phenotype. *J Pediatr* 2009; **155**: 900–903.
33 Wang JC, Passage MB, Yen PH, Shapiro LJ, Mohandas TK: Uniparental heterodisomy for chromosome 14 in a phenotypically abnormal familial balanced 13/14 Robertsonian translocation carrier. *Am J Hum Genet* 1991; **48**: 1069–1074.
34 Kagami M, Yamazawa K, Matsubara K *et al*: Placentomegaly in paternal uniparental disomy for human chromosome 14. *Placenta* 2008; **29**: 760–761.

This work is licensed under a Creative Commons Attribution 3.0 Unported License. The images or other third party material in this article are included in the article's Creative Commons license, unless indicated otherwise in the credit line; if the material is not included under the Creative Commons license, users will need to obtain permission from the license holder to reproduce the material. To view a copy of this license, visit http://creativecommons.org/licenses/by/3.0/

Supplementary Information accompanies this paper on European Journal of Human Genetics website (http://www.nature.com/ejhg)

OPEN

Journal of Human Genetics (2015), 1–8
© 2015 The Japan Society of Human Genetics All rights reserved 1434-5161/15
www.nature.com/jhg

REVIEW

Kagami–Ogata syndrome: a clinically recognizable upd (14)pat and related disorder affecting the chromosome 14q32.2 imprinted region

Tsutomu Ogata[1,2] and Masayo Kagami[2]

Human chromosome 14q32.2 carries paternally expressed genes including *DLK1* and *RTL1*, and maternally expressed genes including *MEG3* and *RTL1as*, along with the germline-derived *DLK1-MEG3* intergenic differentially methylated region (IG-DMR) and the postfertilization-derived *MEG3*-DMR. Consistent with this, paternal uniparental disomy 14 (upd(14)pat), and epimutations (hypermethylations) and microdeletions affecting the IG-DMR and/or the *MEG3*-DMR of maternal origin, result in a unique phenotype associated with characteristic face, a small bell-shaped thorax with coat-hanger appearance of the ribs, abdominal wall defects, placentomegaly and polyhydramnios. Recently, the name 'Kagami–Ogata syndrome' (KOS) has been approved for this clinically recognizable disorder. Here, we review the current knowledge about KOS. Important findings include the following: (1) the facial 'gestalt' and the increased coat-hanger angle constitute pathognomonic features from infancy through childhood/puberty; (2) the unmethylated IG-DMR and *MEG3*-DMR of maternal origin function as the imprinting control centers in the placenta and body respectively, with a hierarchical interaction regulated by the IG-DMR for the methylation pattern of the *MEG3-DMR* in the body; (3) *RTL1* expression level becomes ~2.5 times increased in the absence of functional *RTL1as*-encoded *microRNAs* that act as a *trans*-acting repressor for *RTL1*; (4) excessive *RTL1* expression and absent *MEG* expression constitute the primary underlying factor for the phenotypic development; and (5) upd(14)pat accounts for approximately two-thirds of KOS patients, and epimutations and microdeletions are identified with a similar frequency. Furthermore, we refer to diagnostic and therapeutic implications.
Journal of Human Genetics advance online publication, 17 September 2015; doi:10.1038/jhg.2015.113

INTRODUCTION

Human chromosome 14q32.2 harbors an imprinted region.[1,2] Consistent with this, paternal uniparental disomy 14 (upd(14)pat) results in a unique phenotypic constellation, and maternal uniparental disomy 14 (upd(14)mat) leads to less characteristic but clinically discernible features.[2,3] Upd(14)pat- and upd(14)mat-compatible phenotypes are also caused by epimutations and microdeletions affecting the maternally and paternally derived chromosome 14q32.2 imprinted region, respectively.[2,4–9] However, until recently, there were no pertinent names for the clinically recognizable disorders. Although the terms 'upd(14)pat syndrome' and 'upd(14)mat syndrome' were utilized previously,[5,7] both are apparently inappropriate as 'upd(14) pat/mat syndrome' can be brought about by (epi)genetic mechanisms other than upd(14)pat/mat.[2,4–9]

Recently, the names 'Kagami–Ogata syndrome' (KOS) (OMIM 608149) and 'Temple syndrome' (TS) (OMIM 616222) have been proposed for upd(14)pat/upd(14)mat and related conditions, respectively.[10,11] The syndrome names have been approved by the European Network for Human Congenital Imprinting Disorders (EUCID.net) (www.imprinting-disorders.eu) on the basis of their significant contribution to the elucidation of clinical and molecular characteristics of the two disorders. Here, we review the current knowledge about KOS.

CLINICAL FINDINGS

Patients

After identification of upd(14)pat by Wang *et al.*[12] in 1991, and that of epimutations and microdeletions affecting the 14q32.2 imprinted region of maternal origin by Kagami *et al.*[2] in 2008, a total of 35 Japanese and 18 non-Japanese patients have been identified with KOS, excluding one Japanese patient with a ring 14 chromosome missing multiple nonimprinted genes[2] and including two unpublished Japanese patients with epimutations (Supplementary Table S1). The patients have upd(14)pat, epimutations or microdeletions, and there has been no KOS patient with a single gene mutation or a duplication of the paternally derived 14q32.2 imprinted region. Upd(14)pat and epimutations reported to date are invariably sporadic, whereas microdeletions of variable sizes are identified as a sporadic form or as a familial form transmitted from the mother.

[1]Department of Pediatrics, Hamamatsu University School of Medicine, Hamamatsu, Japan and [2]Department of Molecular Endocrinology, National Research Institute for Child Health and Development, Tokyo, Japan
Correspondence: Professor Tsutomu Ogata, Department of Pediatrics, Hamamatsu University School of Medicine, 1-20-1, Handayama, Higashi-ku, Hamamatsu 431-3192, Japan.
E-mail: tomogata@hama-med.ac.jp
Received 15 June 2015; revised 9 August 2015; accepted 25 August 2015

Phenotypic summary

Comprehensive clinical studies have recently been performed for Japanese patients.[10] The results, in conjunction with clinical findings of non-Japanese patients (Supplementary Table S1), are summarized as follows: (1) phenotypes are similar irrespective of the underlying cause and ethnicity; (2) the facial 'gestalt' with full cheeks and protruding philtrum and the increased coat-hanger angle to the ribs constitute unique pathognomonic features from infancy through childhood/puberty (and probably in adulthood as well) in KOS, and the decreased ratio of the mid to widest thorax diameter (M/W) is also specific to KOS in infancy, although it becomes within the normal range after infancy (Figure 1, Supplementary Figure S1) (facial photographs have also been published in many papers);[10,12–21]

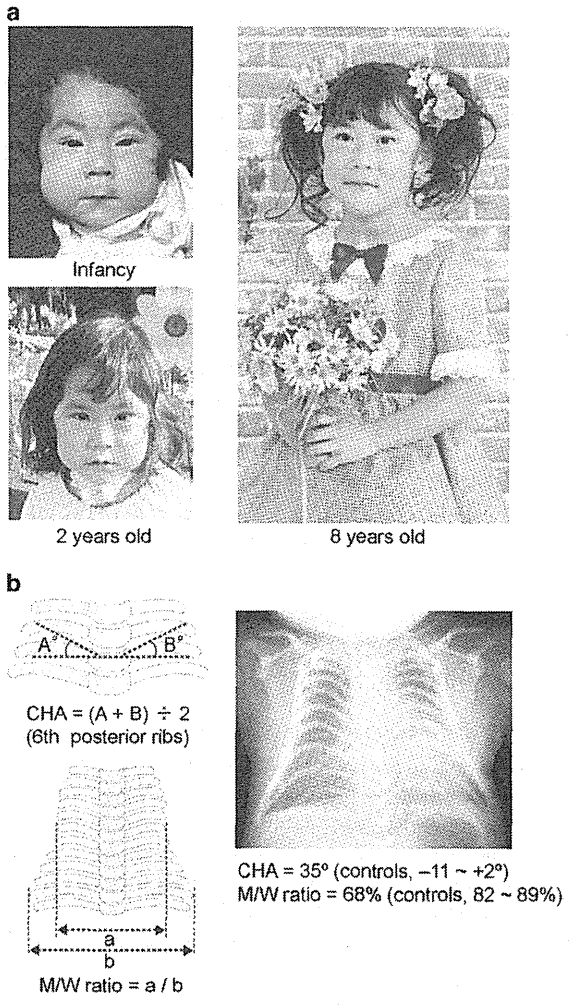

Figure 1 Unique pathognomonic features in Kagami–Ogata syndrome (KOS). **(a)** Photographs of a patient with a maternally inherited 411 354 bp microdeletion involving *DLK1*, the IG-DMR, the *MEG3*-DMR, *MEG3*, *RTL1*/*RTL1as*, *MEG8* and a centromeric part of *snoRNAs* (Deletion-4 in Figure 3).[2] IG-DMR, intergenic differentially methylated region. The facial 'gestalt' with full cheeks and protruding philtrum is observed from infancy through childhood. **(b)** Chest roentgenogram of a hitherto unreported Japanese neonatal patient with an epimutation. The CHA (coat-hanger angle) to the ribs is increased, and the M/W ratio (the ratio of the mid to widest thorax diameter) is decreased. Normal values are based on our previous report.[10]

(3) abdominal wall defects including omphalocele, placentomegaly and polyhydramnios represent characteristic but not specific features in KOS, as they are also observed in several disorders such as Beckwith–Wiedemann syndrome and androgenetic mosaicism;[22,23] (4) KOS is also associated with rather common but important features such as prenatal overgrowth/overweight, developmental delay and feeding difficulties; (5) polyhydramnios is ascribed to placentomegaly and feeding difficulty (impaired swallowing), and the relevance of both placental and body factors explains why polyhydramnios can be present in patients lacking placentomegaly or feeding difficulties; (6) hepatoblastoma has been identified in three infantile patients; and (7) mortality is ~ 30%, and has invariably occurred before 4 years of age.

In addition, two negative findings would also be worth pointing out. First, hypothyroidism has not been described in KOS patients.[2,10] This finding, together with lack of hyperthyroidism in TS patients,[11] would argue against *DIO3* being an imprinted gene, because DIO3 functions as an inactivator of thyroid hormones.[24] Second, there is no KOS patient with diabetes mellitus, although positive associations have been identified between paternally inherited rs941576 in this imprinted region and type I diabetes mellitus[25] and between downregulation of *MEGs* in this imprinted region and type II diabetes mellitus.[26] Thus, the relevance of this imprinted region to diabetes mellitus would be minor, if any.

HUMAN CHROMOSOME 14Q32.2 IMPRINTED REGION

Imprinted genes

This region harbors protein-coding paternally expressed genes (*PEGs*) such as *DLK1* and *RTL1*, and noncoding maternally expressed genes (*MEGs*) such as *MEG3* (alias, *GTL2*), *RTL1as* (*RTL1* antisense), *MEG8*, *snoRNAs* and *microRNAs* (Figure 2a).[1,2] Parent-of-origin-specific expression patterns have been confirmed in somatic and placental cells of control subjects and KOS patients.[2,4,27] For *DIO3*, biparental expression has been indicated at least in the placenta,[27] consistent with lack of thyroid diseases in KOS and TS.[10,11]

Differentially methylated regions (DMRs)

This region also carries the intergenic DMR (IG-DMR) between *DLK1* and *MEG3* and the *MEG3*-DMR at the *MEG3* promoter region (Figure 2a).[2,28] Both DMRs are methylated after paternal transmission and unmethylated after maternal transmission in the body; in the placenta, the IG-DMR alone remains as a DMR, and the *MEG3*-DMR is grossly hypomethylated regardless of parental origin (Figure 2b).[2,4,27] These findings suggest that the IG-DMR is a germline-derived primary DMR, whereas the *MEG3*-DMR is a postfertilization-derived secondary DMR.[1,29]

Imprinting control centers (ICCs)

The *MEG3*-DMR and the IG-DMR of maternal origin function as ICCs in the body and the placenta, respectively, with a hierarchical interaction between the two DMRs in the body (Figure 2b).[4] Indeed, loss of a 4303-bp segment encompassing the unmethylated *MEG3*-DMR of maternal origin has resulted in maternal to paternal epigenotypic alteration (absent *MEG* expression and biparental *PEG* expression) in the body, thereby leading to a typical KOS body phenotype in the presence of the differentially methylated IG-DMR; the placenta was apparently normal, consistent with the non-DMR pattern of the *MEG3*-DMR in the placenta.[4] Similarly, loss of an 8558-bp segment involving the unmethylated IG-DMR of maternal origin has caused maternal to paternal epigenotypic alteration in the placenta and an epimutation (hypermethylation) of the *MEG3*-DMR in the body, thereby leading to typical KOS placental and body

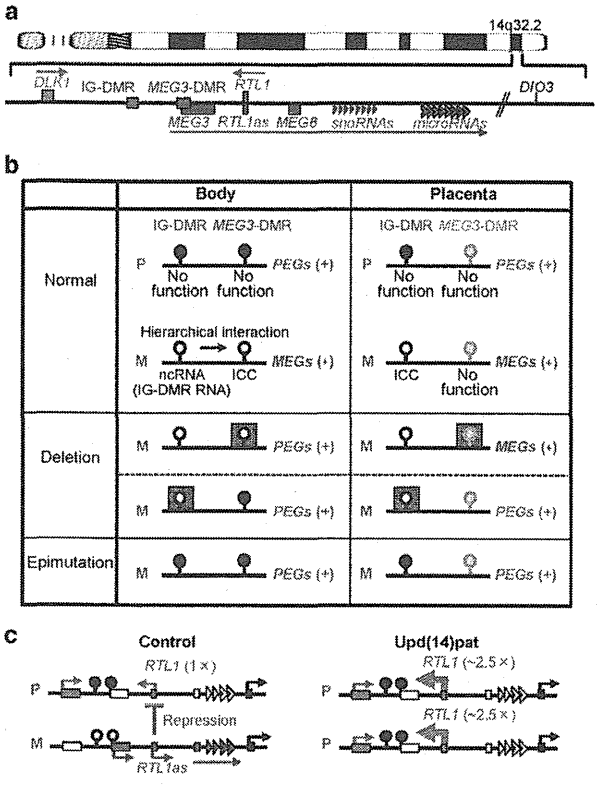

Figure 2 The human chromosome 14q32.2 imprinted region. (**a**) Schematic representation of the physical map of this region. *PEGs* are shown in blue, *MEGs* in red, a probably non-imprinted gene (*DIO3*) in black and the DMRs in green. (**b**) Methylation patterns of the DMRs. Black, white and gray painted circles represent methylated DMRs, unmethylated DMRs and non-DMRs, respectively. The arrow indicates a hierarchical interaction between the IG-DMR and the *MEG3*-DMR that appears to be medicated by *cis*-acting ncRNAs (the IG-DMR RNA) that exerts an enhancer-like function for the *MEG3* promoter and prevents the *MEG3*-DMR from methylation. The deleted regions are shown with stippled squares. (**c**) Interaction between *RTL1* and *RTL1as*. In control subjects, *RTL1as*-encoded *microRNAs* function as a *trans*-acting repressor for *RTL1*. In upd(14)pat patients, *RTL1* expression level becomes ~5 times increased because of two copies of functional *RTL1* and no functional *RTL1as* (shown with thick arrows). DMR, differentially methylated region; ICC, imprinting control center; IG-DMR, intergenic differentially methylated region; M, maternally derived chromosome; *MEGs*, maternally expressed genes; ncRNA, noncoding RNA; P, paternally derived chromosome; *PEGs*, paternally expressed genes; upd(14)pat, paternal uniparental disomy 14.

phenotypes.[4] It is likely that the unmethylated IG-DMR controls the imprinting pattern directly in the placenta, and indirectly in the body by hierarchically regulating the methylation pattern of the *MEG3*-DMR. In this regard, it is postulated that epimutations (hypermethylations) of the IG-DMR of maternal origin also lead to maternal to paternal epigenotypic alterations, as reported in other imprinting disorders (Figure 2b).[3,30] Furthermore, as the epimutations identified in KOS and TS patients have invariably affected both the IG-DMR and the *MEG3*-DMR, with no isolated epimutation of the IG-DMR or the *MEG3*-DMR,[2,6–11] this would be compatible with the notion that the methylation pattern of the *MEG3*-DMR is determined by that of the IG-DMR.

Although it remains to be elucidated how the two unmethylated DMRs of maternal origin function as ICCs with an interaction in the body, significant progress has been made for this issue. It is likely that nearly all *MEGs*, which are transcribed in the same orientation from the forward strand with a strikingly similar tissue expression pattern, comprise a long multicistronic noncoding RNA transcript (Figure 2a),[31,32] and that this transcript is expressed by the *MEG3* promoter at the *MEG3*-DMR in somatic cells and by a different promoter in placental cells. Indeed, it is difficult to postulate a parent-of-origin-specific function for the placental *MEG3* promoter that resides in a rather hypomethylated region irrespective of the parental origin.[2,4,27] Furthermore, Kota *et al.*[33] have shown that the IG-DMR of maternal origin harbors bidirectionally expressed *cis*-acting relatively short (mostly <500 bp and up to 750 bp) noncoding RNAs named the 'IG-DMR RNA' that exerts an enhancer-like function for the *MEG3* promoter as recently identified enhancer RNAs[34,35] and protects the *Gtl2/Meg3*-DMR from *de novo* methylation (Figure 2b). These findings would explain why the *MEG3*-DMR can control nearly all the *MEGs* expression in the body under the hierarchical regulation of the IG-DMR, although it remains unknown how the IG-DMR regulates the *MEG* expression in the placenta. For *PEGs*, the biallelic expression of *DLK1* and absence of noncoding RNA in birds and fish that are free from genomic imprinting imply that the paternal-type imprinting pattern with positive *DLK1* expression is the default situation of this domain.[36,37] Thus, loss or epimutation of the IG-DMR and the *MEG3*-DMR of maternal origin would result in the positive *PEG* expression as the default condition in the placenta and the body, respectively.

For the *MEG3*-DMR, it contains two putative CTCF-binding sites with a DMR-compatible methylation pattern.[1,4,38] Thus, it may be possible that preferential binding of CTCF protein with versatile functions to the unmethylated CTCF-binding sites activates all *MEGs* as a large transcription unit. In addition, as mouse *Gtl2/Meg3*-DMR is associated with parental origin-specific histone acetylation,[39] CTCF protein binding may inhibit all *PEGs* by affecting histone modification.[1,4,38–40] However, although the CTCF protein can bind to the two putative binding sites,[38] previous studies have failed to show a preferential binding of CTCF protein to the unmethylated binding sites.[41] Thus, the relevance of the CTCF-binding sites to the ICC function awaits further investigations.

It should be pointed out that the expression patterns of the 14q32.2 imprinted genes are also influenced by a *trans*-acting factor(s) other than the ICCs. It has recently been shown that IPW, a long noncoding RNA in the Prader–Will syndrome (PWS) critical region, functions as a regulator for the expression of the imprinted genes at chromosome 14q32.2.[42] Thus, the imprinting regulation mechanisms would be much more complex.

RTL1/RTL1as interaction and expression dosage of the imprinted genes

RTL1as-encoded *microRNAs* function as a *trans*-acting repressor for *RTL1* expression (Figure 2c). Actually, quantitative PCR analyses have indicated ~5 times, rather than 2 times, increased *RTL1* expression level in fresh placentas with upd(14)pat, as well as doubled *DLK1* expression level and absent *MEGs* expression.[27] This suggests that the *RTL1* expression level is ~2.5 times increased in the absence of functional *RTL1as*. Immunohistochemical examinations have also identified markedly increased RTL1 protein expression and moderately increased DLK1 protein expression in the vascular endothelial cells and pericytes of chorionic villi with upd(14)pat.[27] The repressive effect of *Rtl1as* on *Rtl1* expression has also been demonstrated in mice.[43,44] No other gene–gene interaction has been demonstrated in this imprinted region.

MAJOR PHENOTYPIC DETERMINANT(S)

Expression dosage of the imprinted genes

Expression patterns in upd(14)pat, epimutations and various microdeletions are shown in Figure 3. Upd(14)pat and epimutations are accompanied by essentially identical expression patterns (that is, 2 times *DLK1* and ~5 times *RTL1* expression dosages, and absent *MEGs* expression), although the possible presence of trisomic cells in trisomy rescue (TR)-type upd(14)pat, that of normal cells in postfertilization mitotic error (PE)-type upd(14) and that of normal cells escaping hypermethylation in epimutations remain possible. In contrast, microdeletions are accompanied by variable expression patterns of the imprinted genes, depending on the size of the deleted regions. Thus, (epi)genotype–phenotype correlations in patients with microdeletions are informative in considering the major phenotypic determinant(s).

(Epi)genotype–phenotype correlations in the body

Body phenotypes are comparable among patients with different causes, and excessive *RTL1* expression (~2.5 times or ~5 times) and absent *MEGs* expression are shared in common (Figure 3 and Supplementary Table S1). In contrast, as patients with Deletions-2 and -4 are associated with typical KOS phenotype in the presence of a normal (1 time) *DLK1* expression dosage, this argues against a major effect of doubled *DLK1* expression dosage on phenotypic development. Thus, there are two possibilities with regard to the major phenotypic determinant(s) in KOS.

First, excessive *RTL1* expression may constitute the major phenotypic determinant(s).[10] In support of this, mouse *Rtl1* is expressed in the fetal ribs, brain and skeletal muscles,[10,45] although assessment of body phenotype remains poor in *Rtl1as* knockout mice, which died within a day, with 2.5–3.0 times *Rtl1* expression.[44] In this case, it is assumed that clinical features are more severe in patients with ~5 times *RTL1* expression than in those with ~2.5 times *RTL1* expression. Although our initial studies supported such an *RTL1* dosage effect on the phenotypic severity,[2] the difference in the *RTL1* expression dosage turned out to have no discernible clinical effects after analyzing long-term clinical courses.[10] This may be explained by assuming the presence of a threshold for the *RTL1* expression level or the buffering effects of multiple genetic and environmental factors for the difference in the *RTL1* expression dosage.

Second, absent *MEGs* expression may play a crucial role in the phenotypic development, independently of the excessive *RTL1* expression resulting from loss of functional *RTL1as*. Indeed, as mouse *Gtl2/Meg3* is expressed in multiple fetal tissues including the primordial cartilage,[46] absent *MEG3* expression may be involved in the phenotypic development. Null expression of *snoRNAs* and/or *miRNAs* may also have clinical effects, as observed in exceptional PWS patients lacking only *snoRNAs* including *SNORD116*.[47] Furthermore, absence of functional IG-DMR RNA may also lead to abnormal phenotypes by affecting the expression patterns of the imprinted genes,[33] although the IG-DMR RNA has not been studied in KOS patients.

The two possibilities are not mutually exclusive, and excessive *RTL1* expression coexists with absent expression of *MEGs* including *RTL1as*. Thus, further studies are required to elucidate which is the more critical determinant. For example, clinical studies in patients with tiny deletions involving maternally inherited *MEG3*, *RTL1as*, *snoRNAs* and/or *miRNAs*, but not the DMRs, will serve to clarify this matter.

(Epi)genotype–phenotype correlations in the placenta

The above notion is also applicable to Deletions-1–4, because Deletions-1–4 are associated with placentomegaly and polyhydramnios, in the presence of excessive *RTL1* expression (~2.5 times or

	Body	Placenta	Phenotype
Control	P *PEGs* 1 X M *MEGs* 1 X	P *PEGs* 1 X M *MEGs* 1 X	Normal
Upd(14)pat (n=37)	P *DLK1* 2 X, *RTL1* ~5 X P *MEGs* 0 X	P *DLK1* 2 X, *RTL1* ~5 X P *MEGs* 0 X	Body: Typical KOS Placentomegaly 83% Polyhydramnios 100%
Epimutation (n=7)	P *DLK1* 2 X, *RTL1* ~5 X M *MEGs* 0 X	P *DLK1* 2 X, *RTL1* ~5 X M *MEGs* 0 X	Body: Typical KOS Placentomegaly 100% Polyhydramnios 100%
Deletion-1 (8,558 bp) (n=1)	P *DLK1* 2 X, *RTL1* ~5 X M *MEGs* 0 X	P *DLK1* 2 X, *RTL1* ~5 X M *MEGs* 0 X	Body: Typical KOS Placentomegaly (+) Polyhydramnios (+)
Deletion-2 (108,768 bp) (n=2)	P *DLK1* 1 X, *RTL1* ~5 X M *MEGs* 0 X	P *DLK1* 1 X, *RTL1* ~5 X M *MEGs* 0 X	Body: Typical KOS Placentomegaly (+) Polyhydramnios (+)
Deletion-3 (474,550 bp) (n=1)	P *DLK1* 2 X, *RTL1* ~2.5 X M *MEGs* 0 X	P *DLK1* 2 X, *RTL1* ~2.5 X M *MEGs* 0 X	Body: Typical KOS Placentomegaly (+) Polyhydramnios (+)
Deletion-4 (411,354 bp) (n=1)	P *DLK1* 1 X, *RTL1* ~2.5 X M *MEGs* 0 X	P *DLK1* 1 X, *RTL1* ~2.5 X M *MEGs* 0 X	Body: Typical KOS Placentomegaly (+) Polyhydramnios (+)
Deletion-5 (165,153 bp) (n=1)	P *DLK1* 2 X, *RTL1* ~2.5 X M *MEGs* 0 X	P *DLK1* 1 X, *RTL1* ~2.5 X M *MEGs* 0 X	Body: Typical KOS Placentomegaly (–) Polyhydramnios (+)
Deletion-6 (5,823 bp) (n=2)	P *DLK1* 2 X, *RTL1* ~5 X M *MEGs* 0 X	P *DLK1* 1 X, *RTL1* 1 X M *MEGs* 1 X	Body: Typical KOS Placentomegaly (?) Polyhydramnios (+)
Deletion-7 (4,303 bp) (n=1)	P *DLK1* 2 X, *RTL1* ~5 X M *MEGs* 0 X	P *DLK1* 1 X, *RTL1* 1 X M *MEGs* 1 X	Body: Typical KOS Placentomegaly (–) Polyhydramnios (–)

Figure 3 Expression patterns of the imprinted genes and methylation patterns (modified from our previous report).[10] For explanations, see the legend for Figure 2. *MEG3* is not expressed in Deletions-6–7, because *MEG3* exons 1–3 are deleted.

~5 times), normal or doubled *DLK1* expression and absent *MEGs* expression in the placenta (Figure 3 and Supplementary Table S1). In particular, excessive *RTL1* expression would play a crucial role in the development of placental features, because *Rtl1as* knockout mice have placentomegaly (~150%) in the presence of 2.5–3.0 times *Rtl1* expression and apparently normal expression of other imprinted genes in this domain.[44]

For the placental phenotype, two findings should be pointed out. First, Deletion-5 was free from placentomegaly,[5] although ~2.5 times *RTL1* expression dosage and absent expression of nearly all *MEGs* are predicted in the placenta as well as in the body (Figure 3). However, this would not pose a major problem, because placentomegaly is not an invariable feature even in patients with upd(14)pat with ~5 times *RTL1* expression dosage and null *MEG* expression. In this context, polyhydramnios in the patient with Deletion-5 would primarily be because of defective swallowing of amniotic fluid, as indicated by the presence of feeding difficulties.[5]

Second, the two siblings with Deletion-6 had polyhydramnios, whereas the patient with Deletion-7 apparently had neither placentomegaly nor polyhydramnios, despite the similar deletion sizes (the deletion size according to hg19: Deletion-6, Chr14: 101 291 322–101 297 145 bp; and Deletion-7, Chr14:101 291 225–101 295 527 bp) (Figure 3).[4,5] As *MEGs* in the placenta would be transcribed by a *cis*-acting promoter other than the *MEG3* promoter in the presence of the IG-DMR, the placentas with Deletions-6 and -7 are predicted to be accompanied by normal expression levels of most *MEGs* including *RTL1as*, except for *MEG3* that is disrupted by the microdeletions, and normal expression levels of *PEGs* including *RTL1*. This notion explains lack of placentomegaly and polyhydramnios in Deletion-7, and excludes a positive role of *MEG3* deficiency in the development of aberrant placental phenotype. For Deletion-6, polyhydramnios would be explained by body factors, because one of two siblings with Deletion-6 manifests feeding difficulty and both siblings have muscular hypotonia that can cause polyhydramnios.[5,48] In addition, placentomegaly is not described in the two siblings with Deletion-6, although no description of a particular phenotype does not necessarily indicate the lack of a corresponding phenotype.

UNDERLYING FACTORS FOR KOS AND UPD(14)PAT

Underlying causes for KOS

Relative frequency of underlying causes is shown in Table 1. Upd(14)pat accounts for approximately two-thirds of KOS patients, and epimutations and microdeletions are identified with a similar frequency. Notably, upd(14)pat has predominantly been found in Japanese patients with normal karyotype and in non-Japanese patients with abnormal karyotype. This would primarily be because of the difference in molecular methods employed before and after the identification of the DMRs.[2] Indeed, Japanese patients have been found by methylation analysis of the DMRs that is carried out irrespective of the karyotype, whereas non-Japanese patients have primarily been detected by genotyping analysis that is preferentially performed for chromosomal abnormalities as a risk factor for upd(14)pat.[49] This notion would also explain why epimutations have been found in Japanese patients only.

The relative frequency is similar to that observed in TS,[11] but is different from that in other imprinted disorders. For example, microdeletions at chromosome 15q11.2–q13 imprinted region are most frequent in PWS and Angelman syndrome, and epimutations of the *H19*-DMR and the KvDMR1 at chromosome 11p15 are most prevalent in Silver–Russell syndrome and Beckwith–Wiedemann syndrome, respectively.[3,30] Although the preponderance of microdeletions in PWS/Angelman syndrome is explained by the presence of low-copy repeats flanking the imprinted region,[50] it is unknown why upd and epimutations are predominant in KOS/TS and Silver–Russell syndrome/Beckwith–Wiedemann syndrome, respectively.

Table 1 Underlying factors for Kagami–Ogata syndrome and upd(14)pat

	Japanese (*n*=35)	*Non-Japanese* (*n*=18)	*Total* (*n*=53)
Underlying causes for KOS			
Upd(14)pat	23	14	37
Normal karyotype	20	5	25
Abnormal karyotype	3	9	12
Epimutation	7[a]	0	7
Microdeletion	5[b]	4[c]	9
Underlying mechanisms for upd(14)pat			
Normal karyotype			
TR/GC	7	0	7
MR/PE	12	2	14
PE	1	2	3
No detailed information	0	1	1
Abnormal karyotype			
Robertsonian translocation	2[d]	3[e]	5
Isochromosome for 14q	0	5[f]	5
Unknown/other karyotype	1	1[g]	2

Abbreviations: GC, gamete complementation; KOS, Kagami–Ogata syndrome; MR, monosomy rescue; PE, postfertilization mitotic error; TR, trisomy rescue; upd(14)pat, paternal uniparental disomy 14.
[a]Including two hitherto unreported patients.
[b]Including sibling cases; thus, four microdeletions have been found in five patients.
[c]Including sibling cases; thus, three microdeletions have been detected in four patients.
[d]45,XX,rob(13;14)(q10;q10) (*n*=1) and 45,XX,rob(14;21)(q10;q10q) (*n*=1); parental karyotype has not been examined.
[e]45,XX,rob(13;14)(q10;q10) (*n*=3); the same Robertsonian translocations have been found in the fathers of the three patients.
[f]45,XX,i(14q) (*n*=4) and 45,XY,i(14q) (*n*=1); parental karyotypes are invariably normal in the five patients.
[g]46,XX[6]/47,XX,+mar[44]. Although the marker chromosome is derived from chromosome 14, it does not involve the 14q32.2 imprinted region, and full isodisomy for chromosome 14 has been shown by microsatellite analysis.

Underlying mechanisms for upd(14)pat

Upd(14)pat is frequently identified in patients with normal karyotype (Table 1). Upd(14)pat in such patients is primarily caused by TR, gamete complementation, monosomy rescue (MR) and PE.[30] TR/gamete complementation is accompanied by at least one heterodisomic locus, MR by full isodisomy and PE by full or segmental isodisomy.[30] In this regard, the predominance of MR/PE-type upd(14)pat in Japanese patients would be related to the recent increase in the maternal childbearing age,[51] because MR-type upd(14)pat is mediated by a nullisomic oocyte that is produced by maternal age-dependent nondisjunction at meiosis 1 as well as by maternal age-independent nondisjunction at meiosis 2.[52] Indeed, maternal childbearing age is significantly increased in Japanese patients with MR/PE-type upd(14)pat.[30] Consistent with this, maternal childbearing age is also significantly advanced in PWS patients with MI nondisjunction-mediated TR/gamete complementation-type upd(15)mat.[51]

Upd(14)pat is also found in patients with abnormal karyotype (Table 1). The Robertsonian 13q;14q translocations in three non-Japanese patients with hetero-upd(14)pat were transmitted from their fathers to the patients,[12,13,53] although Robertsonian translocations